Goethe Universität Frankfurt
Institut für Theoretische Physik

Master Thesis

Mean Field Approach to Effective Polyakov Loop Theories

Vinzenz M. Wiedemann

Supervisor and first referee: Prof. Dr. Owe Philipsen

Second referee: Prof. Dr. Marc Wagner

December, 2019

Zusammenfassung

In dieser Arbeit werden verschiedene Polyakov Loop Theorien mit Hilfe einer mean field Analyse untersucht. Der Polyakov Loop ist eine Observable der Gitter-Quantenchromodynamik bei endlichen Temperaturen, der im Falle unendlich schwerer Quarks einen Ordnungsparameter des deconfinement Phasenübergangs darstellt. Die Theorien sind hierbei effektive Modelle der Quantenchromodynamik, die direkt aus dieser hergeleitet werden. Die mean field Analyse stellt einen analytischen Zugang dar, über den sich das qualitative Verhalten der Theorien untersuchen lässt. Insbesondere beim Deconfinement Übergang wird auf unterschiedliche Einflüsse eingegangen. Dazu zählen unter anderem die Auswirkungen schwerer Quarks, die zunächst statisch und später auch dynamisch eingeführt werden. Zudem wird die Änderung des Phasenübergangs bei imaginärem chemischen Potential untersucht. Schließlich wird der Übergang bei endlichem chemischen Potential in der Annahme von schwerer und dichter Quarkmaterie vom Hadronengas zu Nukleonen untersucht.

Abstract

In this thesis we study various Polyakov loop models with mean field theory. The Polyakov loop is an observable of finite-temperature lattice quantum-chromodynamics. It is an order parameter for the deconfinement phase transition in the case of infinitely heavy quarks. The Polyakov loop theories are effective models, which are directly derived from quantum-chromodynamics. The mean field approach allows for an analytic access. Thus, we can study the qualitative behavior of the theory. The deconfinement phase transition is studied for different cases. These include the effects of heavy quarks, which are initially introduced statically and later dynamically. In addition, the change of the phase transition at imaginary chemical potential is investigated. Finally, the liquid-gas transition of nuclear matter at finite chemical potential in the assumption of heavy and dense quark matter is studied.

Contents

1 Introduction

The strong interaction is one of the four fundamental forces of the universe. Together with the electromagnetic and the weak interaction it forms the Standard Model of particle physics. Only gravity is not yet included in a "theory of everything". The Standard Model is described by quantum field theories. The theory of the strong force is called quantum chromodynamics (QCD). A quantum field theory is a microscopic theory which combines quantum mechanics with special relativity and utilizes many aspects of statistical physics. Since quantum field theories are many-body theories one can evaluate the thermodynamic properties of them. The interactions are characterized by their symmetries with respect to their gauge group. The Standard Model contains 24 fermions which are devided into six quarks and six leptons plus their antiparticles. On the other hand, it also contains several bosons which act as charge carriers.
The elementary particles of QCD are the quarks which form hadrons like the proton or the neutron. There are six different quark flavors: up, down, strange, charm, top and bottom. They are coupled to the QCD charge which is called color charge. This color charge is carried by the eight gauge particles of QCD. They are called gluons. The theory obeys some symmetries. This means that the Lagrangian of the theory is invariant under certain transformations. The gauge group of QCD is SU(3).
QCD exhibits two important features. At low energies confinement appears. This means that color charged particles form hadrons and can not be isolated. In contrast, at high energies the coupling weakens and the quarks and gluons are quasi free and form the quark-gluon plasma. In this regime QCD is asymptotically free.
Since the coupling constant is large at low temperatures, a perturbative treatment of the theory is impossible in this regime. Therefore, a lot of effort has been taken to develop different approaches to gain a better insight into the theory. One of the main questions to this day is if QCD exhibited phase transitions. Phase transitions are closely related to a symmetry breaking. We take a closer look at phase transitions in section 2.
The QCD phase diagram has a tremendous importance for physics. In the QCD phase diagram the state of the system is expressed in the space of thermodynamic quantities. These are typically the temperature T and the chemical potential μ. Due to its hard mathematical access, its detailed look especially at finite densities is quite unknown. QCD has a wide range of applications. One is cosmology since it is important for understanding processes which occurred shortly after the big bang in the early universe. There are also some experimental tests which can be studied in collision experiments. The high density region has importance for astrophysics since this state of nuclear matter can be realized in compact objects like neutron stars.
Lattice QCD (LQCD) is a very powerful tool to get non-perturbative access to QCD. The main idea is to discretize space-time on a four-dimensional lattice. The theory can then be evaluated numerically with Monte-Carlo methods. A short overview of the lattice formulation of QCD is given in section 3.1.
Nevertheless, it is not possible to explore the finite density region with LQCD due to the sign problem at finite chemical potential. Importance sampling methods, which are essential for the numerical evaluation, fail because the integrant starts to oscillate. Therefore, one has to find effective theories. Those theories make certain assumptions.

The effective theory used in this thesis is directly derived from LQCD and will be discussed in section 3.
In this thesis we will derive a mean field method to evaluate the effective theory. Then we will use Landau's theory of phase transition to look for the deconfinement phase transition in pure gauge theory. We study the effects of fermions on this phase transition by introducing the static fermion determinant in the hopping parameter expansion. We will extend the mean field approach to higher orders in the hopping parameter and compare the results to numerical computations and the spin model. The region of imaginary chemical potential is discussed and finally indications for the liquid-gas transition of nuclear matter are explored.
In this thesis we restrict ourselves to the number of colors $N_c = 3$ and the number of flavors $N_f = 1$. In principle it is possible to extend the effective theory to other gauge groups and include more quark flavors.

2 Phase transitions and order parameters

The state of strong interacting matter changes with temperature and density. At low temperature, quarks and gluons form hadrons while at high temperatures they are asymptotically free. There, they form the quark-gluon plasma. Since both states are quite different a phase transition has to occur between them.
In general, phase transitions are categorized into three different types. They are characterized by the behavior of their order parameter η. The order parameter is a macroscopic quantity which changes in a certain way at the transition. It describes the state of the system and is associated with the symmetry which is broken at the phase transition. An order parameter is not unique. Every quantity which satisfies the following criterion can be used as an order parameter.

$$\eta = \begin{cases} 0 & \text{symmetric phase} \\ \neq 0 & \text{symmetry-broken phase} \end{cases} \tag{2.1}$$

Phase transitions are categorized by Landau in the following way:

1. First order phase transition
2. Second order/ continuous phase transition
3. Crossover

For the first type of phase transitions the order parameter is discontinuous. This indicates a coexistence of two phases at the phase boundary. A prominent example of a first order phase transition is the boiling of water or the melting of ice. The transition point is defined as the point where it becomes energetically favorable to change the state of the system. A first order transition involves latent heat. This indicates that the temperature stays constant while energy is added to or removed from the system.
For the second type of phase transitions the order parameter changes continuously from zero to s finite value. For these types of phase transitions quantities like the correlation length diverge at the transition. The divergence shows some universal behavior which does not depend on the microscopic details of the system. The denomination roots back to the Ehrenfest classification which classified phase transitions by a discontinuity in the n^{th} derivative of the free energy. This turned out to be wrong since for second order transitions the susceptibility is not discontinuous but diverges. Due to this they are also called continuous phase transitions.
The last type is a crossover. Technically, the crossover is not a real phase transition. It is smooth and does not involve any non-analyticities. It does not show any discontinuities in the free energy or its derivatives although the state of the system changes drastically. This would correspond to a phase transition of infinite order in Ehrenfest's classification. For this type of transition, the boundary between two different states is smeared out. One cannot tell where one phase ends and the other starts.
For first and second order phase transitions, two phases are separated by a clear boundary. This boundary can end in a critical point. An example is the liquid-gas transition. At the critical point the first order phase transition turns into a second order transition. Afterwards the boundaries disappear and the transition becomes a crossover.

These categorizations are closely connected to a symmetry breaking in the system. In pure gauge theory the symmetry which is spontaneously broken is the center symmetry. This symmetry will be discussed in section 3.5.
The order parameter for the confinement-deconfinement phase transition is the Polyakov loop. It is only an exact order parameter for pure gauge theory. Even if the symmetry of the phase transition is roughly realized the order parameter can still be used as an indicator for a phase change in the system.

2.1 Symmetry breaking

A phase transition is closely related to a spontaneous symmetry breaking. The symmetry is broken in one phase and restored in the other phase. This is described by the order parameter that is zero in the phase where the symmetry is restored and non-zero else. This corresponds to the fact that the system cannot change symmetry continuously. Two states of distinct symmetry have to be separated by a phase boundary. This is known as Landau's symmetry principle. Nevertheless, this does not describe how the transition occurs. The order of the transition can still be different for distinct systems.
In pure gauge theory this symmetry is the center symmetry which will be explained in section 3.5. The corresponding order parameter is the Polyakov loop.
Besides spontaneous symmetry breaking, which is associated with a phase transition, a symmetry can also be explicitly broken. If the Lagrangian of the system and hence the equations of motion were not invariant under a certain transformation, the corresponding symmetry is explicitly broken. Even in a system where a symmetry is explicitly broken, spontaneous symmetry breaking can occur. The order parameter can nevertheless be used to signal a phase transition. At a certain point the symmetry of both states can not be distinguished anymore. This is where a crossover is realized.

2.2 Mean field theory

Mean field theory is a method used in statistical physics. Instead of evaluating the whole microscopic theory, one approximates the interactions in the theory with a mean field $\bar{\phi}$. This reduces the many-body problem which can be computationally costly to an effective one-body problem. This is much easier to evaluate and one can extract certain characteristics of the system. Additionally, it allows for an analytic access to the theory. The term mean field theory summarizes a whole class of approximation schemes. In the following we will present a short overview over the method used in this work. For other mean field approaches we refer to [1]. Mean field theory forms the basis for Landau's theory of phase transition which will be discussed later. The derivation of the mean field approach for the effective theory is found in section 4.
The effective Polyakov loop theory can be treated as a many-body problem, where the spins ϕ_i are somehow coupled to their neighbors ϕ_j. The partition function will contain

terms which look like

$$\begin{aligned} &\int [d\phi] \prod_{\langle ij \rangle} e^{f(\phi_i \phi_j)}, \\ &[d\phi] = \prod_{i=1}^{n} d\phi_i, \end{aligned} \tag{2.2}$$

where f is a function of the fields and n is the total number of fields. The simplest form would be a constant factor. Evaluating these integrals is very challenging since in realistic systems n goes to infinity. With mean field theory we decouple these interaction terms. Therefore, the fields ϕ_i and ϕ_j can be replaced by a mean value plus a fluctuation term which still has a spatial dependence $\phi_i = \bar{\phi} + \delta\phi_i$. The mean value is just a number and does not depend on any field. Thus, it can be factored out of the integral. Now we assume that this fluctuation term $\delta\phi$ is small. Hence, only terms of $\mathcal{O}(\delta\phi)$ are kept. This implies that the field varies only very smoothly over the whole system. Next, we resubstitute $\delta\phi_i = \phi_i - \bar{\phi}$. As a result all fields in the system are decoupled and the integral factorizes.

$$\int [d\phi] \prod_{i} e^{g(\bar{\phi})\ \phi_i + \mathcal{O}(\delta\phi^2)} \tag{2.3}$$

$g(\bar{\phi})$ is now a function which only contains the mean field and does not depend on the different fields. The partition function is now easy to evaluate since all fields contribute equally. Finally, the mean field has to be determined. This can be done self-consistently by fixing it to the expectation value of the field ϕ. Thus the self-consistency condition is given as

$$\bar{\phi} = \langle \phi \rangle. \tag{2.4}$$

This method can be easily generalized to a version with multiple independent fields. This is the case in the effective Polyakov theory used in this thesis. The gauge group SU(3) has a fundamental and an anti-fundamental representation. Thus, there is also a complex conjugate of the Polyakov loop. Later we will treat $\bar{\phi}$ and $\bar{\phi}^*$ as independent variables. There are a lot of similarities with spin models, which have been studied in detail. Since a Polyakov loop is a trace over SU(3) matrices, it can be interpreted as a spin with a continuous complex value.

2.3 Landau's description of phase transitions

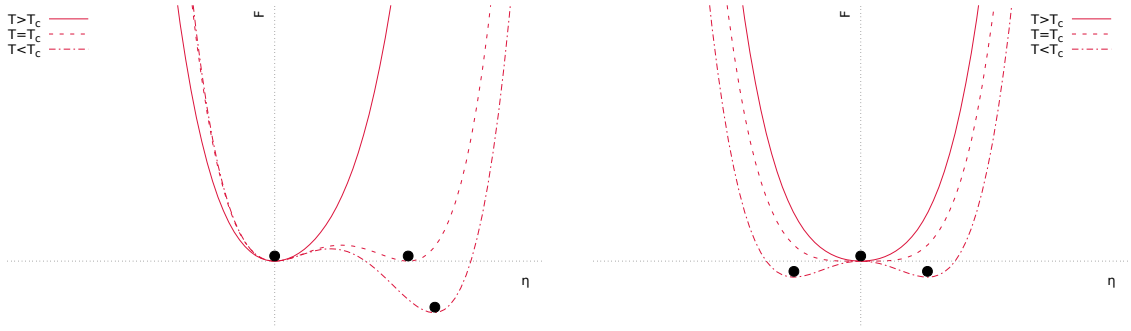

(a) First order phase transition (b) Second order phase transition.

Figure 1: Schematic illustration of phase transitions with Landau's theory of phase transitions. The state of the system is given by the global minimum of the free energy.

Lev Landau developed a continuous theory to describe phase transitions. Landau's theory is based on mean field theory. It postulates that the free energy can be expanded in terms of an order parameter η close to the phase transition. This is legitimate since the order parameter is zero in the disordered phase and shifts smoothly to non-zero values at the transition point in the case of a continuous phase transition. The free energy can then be written as:

$$F(\eta) = \sum_{n=0}^{\infty} a_n[T, \beta]\ \eta^n \tag{2.5}$$

Note that the expansion coefficients are now dependent on the temperature T and the coupling constants β of the system. The equilibrium state of the system is then given as the global minimum of the free energy. In the disordered phase it is at $\eta = 0$. If the system has a symmetry for $\eta \to -\eta$ all odd labeled coefficients are zero and we can write F up to $\mathcal{O}(\eta^4)$ as

$$\frac{\partial F}{\partial \eta} = 2a_2\ \eta + 4a_4\ \eta^3 \stackrel{!}{=} 0. \tag{2.6}$$

This has only the trivial solution for a_2 and a_4 larger zero but at the critical coupling β_c where a_2 changes its sign the minimum shifts to a non-zero value. This is the behavior of a continuous phase transition. As a consequence the phase transition corresponds to a symmetry breaking since the global minimum is not invariant under the symmetry. Despite describing continuous phase transitions Landau's theory can also be used to describe first order phase transitions. Therefore, one has to consider a more general version of the free energy where we allow coefficients of odd exponents to be non-zero. The cubic term of the order parameter is of particular interest. Consider the free energy

$$F = a\ \eta^2 + b\ \eta^3 + c\ \eta^4. \tag{2.7}$$

Besides the trivial solution $\eta_1 = 0$ it has also an extremum at

$$\eta_{2/3} = -\frac{3b}{8c} \pm \sqrt{\left(\frac{3b}{8c}\right)^2 - \frac{a}{2c}} \tag{2.8}$$

This becomes relevant if $\eta_{2/3} \in \mathbb{R}$. This holds for $a \leq \frac{9b^2}{32c}$. From this point on a new minimum and maximum has developed. By further decreasing a the new minimum will shrink, too. At a certain point the global minimum which was so far at $\eta = 0$ gets degenerate. Here, the order parameter, who characterizes the state of the system, will discontinuously "jump" from the global minimum at zero to the non-zero value. This corresponds again to a spontaneous symmetry breaking. This is illustrated in figure 1a. It is important to notice that at the point where the order parameter is non-zero the primary assumption for Landau theory is in general not true since the order parameter is no longer small. Hence, Landau theory is in general not valid anymore [1]. Regardless, it is possible to describe first order phase transitions qualitatively.
In the previous example the order parameter was assumed to be homogeneous, i.e. η does not have any spacial or temporal dependence. In general this is not the case and one has to calculate the expectation value of the order parameter. Also the order parameter does not have to be a scalar in general. As we will see later, the order parameter can have more than one component. The Landau free energy is then constructed out of a combination of the components of the order parameter.

3 From QCD to an effective theory

In the following we will shortly explain some theoretical features of QCD and how to derive the effective theory used in this thesis. For a more detailed overview take a look at [2, 3].
As mentioned before, quantum chromodynamics (QCD) is the theory which describes the strong force. QCD is a non-abelian gauge theory which is invariant under local SU(3) color transformations. The Lagrangian is given as

$$\mathcal{L}_{\mathrm{QCD}} = \sum_{c,f} \overline{\psi}_{cf}(i\gamma^\mu D_\mu - m_f)\psi_{cf} - \frac{1}{4}F^a_{\mu\nu}F^{a\mu\nu}, \tag{3.1}$$

where c and f are the color and flavor indices, ψ the quark spinor, D_μ the covariant derivative, m_f the quark masses and $F^a_{\mu\nu}$ the field strength tensor which contains the gluon fields.

$$D_\mu = \partial_\mu - igA^a_\mu T^a \tag{3.2}$$

$$F^a_{\mu\nu} = \partial_\mu A^a_\nu - \partial_\nu A^a_\mu + g f_{abc} A^b_\mu A^c_\nu \tag{3.3}$$

The first term in equation 3.1 contains the quark contributions while the second term, also referred to as Yang-Mills term, describes the dynamics of the gluon (gauge) fields. g is the QCD coupling constant. In contrast to QED it is not small at low energies which makes a perturbative treatment of the theory impossible in this regime.
Besides the local SU(3) symmetry some other symmetries are conserved. One is the U(1) baryon number conservation. There are some additional symmetries which are only approximately conserved. One is the $SU(N_f)$ flavor symmetry which is only true for degenerate quark masses. This is approximately true for the up and down quark since $m_u \approx m_d$. Chiral symmetry is realized for vanishing quark masses ($m_f = 0$).
With this Lagrangian it is possible to express transition amplitudes of field configurations with the Feynman path integral formalism.

$$\langle\psi_1|e^{-iH(t_2-t_1)}|\psi_2\rangle \sim \int [dA][d\psi][d\overline{\psi}] \exp\left(i \int d^4x\ \mathcal{L}[A,\psi,\overline{\psi}]\right) \tag{3.4}$$

The integration measure represents an integration over all possible field configurations with ψ_1 and ψ_2 as boundary conditions. Although this path integral is not well defined in the continuum, it is computable on a finite lattice. One reason is that the integral measure is only defined for a finite value of field configurations and since the integrant is oscillating the integral does not converge in general.
The exponent of the path integral is called action. It is the integral over the Lagrangian.

$$S = \int d^4x\ \mathcal{L} \tag{3.5}$$

One can see that it is possible to link this transition amplitude to statistical physics. Therefore, one has to perform a Wick rotation. This is done by rotating Minkowski space-time to Euclidean space-time.

$$t \to -i\tau \qquad S \to iS_{\mathrm{E}} \tag{3.6}$$

The similarity between this Euclidean path integral and the grand canonical partition function is now obvious. The grand canonical partition function is given as

$$Z = \mathrm{tr}\left[\exp\left(-\beta(H-\mu N)\right)\right], \tag{3.7}$$

where β is the inverse temperature and H the Hamiltonian. This exactly matches the form of the path integral from equation 3.4 after the Wick rotation. The partition function is then expressed in terms of a path integral.

$$Z = \int [dA][d\psi][d\overline{\psi}] e^{-S_{\mathrm{E}}} \tag{3.8}$$

Notice that gauge fields are represented in terms of complex numbers while the fermions are represented by Grassmann valued fields. Additionally, one has to include the chemical potential μ. It is coupled to the corresponding particle number N. The temperature is included by keeping the time extent finite. The Euclidean action reads

$$S_{\mathrm{E}} = \int_0^{\frac{1}{T}} d\tau \int d^3x\ \overline{\psi}(\gamma_\mu(\partial_\mu + igA_\mu) + m + \gamma_4\mu)\psi + \frac{1}{4}F^a_{\mu\nu}F^a_{\mu\nu}. \tag{3.9}$$

From here on one can compute all expectation values of the system in equilibrium.

3.1 Lattice QCD

Lattice QCD is a method to extract physical information from the path integral in a mathematically well defined way. Therefore, one discretizes space-time on a 4-dimensional lattice Λ with lattice spacing a. The spatial extent is referred to as N_s while the temporal extent is referred to as N_τ. The total number of lattice points is then given as $N_s^3 N_\tau$. Since the lattice spacing a introduces a smallest distance it acts as a UV regulator. To calculate integrals over elements of a gauge group, one has to introduce the correct measure. This measure has to be invariant under gauge transformations. This measure is called Haar measure and can be computed by demanding gauge invariance for the individual measure. Physical quantities are then derived by extrapolating the results to the continuum limit ($a \to 0$).
It is important to mention that the temperature is related to the temporal lattice extent ($T = 1/(N_\tau a)$). It is common to use periodic boundary conditions. They have to be chosen with care. Since fermions have spin 1/2 and obey the Pauli principle the fermion fields are anti-periodic in temporal direction and periodic in spatial direction. This reflects their statistical properties. Due to the relation to temperature they are important to consider although they vanish for $T \to 0$.
To evaluate QCD on the lattice we first have to formulate a lattice version of the QCD Lagrangian. Hence, it is useful to introduce the concept of the gauge link $U_\mu(x)$.

$$U_\mu(x) = e^{-igaA_\mu} \quad \in SU(3) \tag{3.10}$$

This object connects neighboring lattice sites. The action is now expressed in terms of gauge variables. Integrating over link variables rather then gauge fields has the advantage that no gauge fixing is necessary. Since the Lagrangian needs to be gauge

invariant one has to construct a gauge invariant quantity from the gauge links. The simplest one is the plaquette $U_{\mu\nu}(x)$. It is a closed loop of four connected links.

$$U_{\mu\nu}(x) = U_\mu(x)U_\nu(x+\hat{\mu})U_\mu^\dagger(x+\hat{\nu})U_\nu^\dagger(x) \tag{3.11}$$

Form here, it is easy to build the Wilson gauge action.

$$S_g[U] = \frac{\beta}{6}\sum_{x\in\Lambda}\sum_{\mu\neq\nu=0}^{3} \text{Re Tr}\left[1 - U_{\mu\nu}(x)\right], \tag{3.12}$$

Thus, the Wilson gauge action is a sum over traces of plaquettes where $\beta = 6/g^2$ is the inverse lattice coupling. It is easy to show that this action converges to the Yang-Mills action in the continuum limit.
It turns out to be far more complicated to get a discretized version of the fermionic part of the QCD Lagrangian. There are several ways of doing so, but all come with some drawbacks. One way of doing so are the Wilson fermions. Their disadvantage is that they break chiral symmetry explicitly. The Wilson-Dirac action reads:

$$\begin{aligned} S_f^W[U,\overline{\psi},\psi] = \overline{\psi}_f(x)\Bigg(-\frac{1}{2a}\sum_{\mu=0}^{3}[(1-\gamma_\mu)U_\mu(x)\delta_{x,y-\hat{\mu}} + (1+\gamma_\mu)U_{-\mu}(x)\delta_{x,y+\hat{\mu}}] \\ + \left(m_W + \frac{4}{a}\right)\delta_{x,y}\Bigg)\psi_f(y). \end{aligned} \tag{3.13}$$

The Wilson action introduces an artificial term which decouples the unwanted doublers. They are additional poles in the fermion propagator due to lattice artifacts. However, chiral symmetry is explicitly broken by this term. By rescaling the fields $\psi = \psi'/\sqrt{2\kappa}$ one ends up in the hopping parameter representation which will be used later on.

$$S_g^f[U,\overline{\psi},\psi] = \overline{\psi}_f(x)Q(x,y)\psi_f(y) \tag{3.14}$$

$$\begin{aligned} Q(x,y) = \delta_{x,y} - \kappa\sum_{\mu=1}^{3}[(1-\gamma_\mu)U_\mu(x)\delta_{x,y-\hat{\mu}} + (1+\gamma_\mu)U_{-\mu}(x)\delta_{x,y+\hat{\mu}}] \\ -\kappa\left[e^{-\mu}(1-\gamma_4)U_4^\dagger(x)\delta_{x,y-\hat{4}} + e^{\mu}(1+\gamma_4)U_4(x)\delta_{x,y+\hat{4}}\right] \end{aligned} \tag{3.15}$$

$$\kappa = \frac{1}{2m_W a + 8}. \tag{3.16}$$

κ is the hopping parameter. As mentioned before the quark fields are represented by Grassmann variables and can be evaluated. This is know as the quark determinant:

$$\int d^n\overline{\psi}d^n\psi \;\; \exp\left[-\sum_{i,j}\overline{\psi}_i Q_{ij}\psi_j\right] = \det[Q] \tag{3.17}$$

Here, it is important to mention that a finite chemical potential μ leads to a complex quark determinant. This is known as the sign problem and results in a failure of the important sampling method which is essential for the numerical evaluation. Notice that for large quark masses m_W, the hopping parameter is small. Thus, one can expand the

quark determinant in κ in this limit.
From here on, it is possible to formulate the path integral for full QCD just in terms of integrals over gauge fields.

$$Z = \int [dU] \det[Q[U]] e^{-S_g[U]} \tag{3.18}$$

$$[dU] = \prod_x \prod_{\mu=0}^{3} dU_\mu(x) \tag{3.19}$$

3.2 Polyakov loop

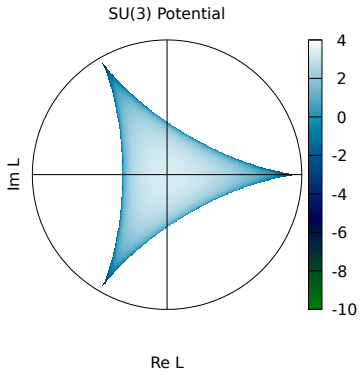

Figure 2: The restricted area for the Polyakov loops L for SU(3) in the complex plain.

Before we introduce the effective theory, we want to introduce the Polyakov loop. In the previous section we presented the plaquette as gauge invariant quantity on the lattice. All connections of link variables which form a closed loop are in principle gauge invariant. All physical observables need to be gauge invariant. One, which can be interpreted as a static color source, is the Polyakov loop. It is sometimes called thermal Wilson line. It is a trace of a closed loop in temporal direction. Thus, it has the maximal temporal lattice extent and is closed via periodic boundary conditions. Hence, it is not closed in a trivial way but winds around the temporal lattice extent. This is the reason why it is not invariant under center transformations. Since the Polyakov loop is a trace over SU(3) matrices it is restricted to a certain domain in the complex plain shown in figure 2. The Polyakov loop is defined as

$$L(\vec{x}) = \mathrm{tr}[T(x, N_\tau)] \coloneqq \mathrm{tr}\left[\prod_{t=0}^{N_\tau - 1} U_0(\vec{x}, t)\right]. \tag{3.20}$$

It is an important quantity in pure gauge theory since its expectation value is related to the free energy of two static color sources [3].

$$|\langle L \rangle| \sim e^{-F/T} \tag{3.21}$$

If the expectation value of the Polyakov loop is zero, an infinite amount of energy is needed to separate the color source. Hence, two static quarks can not be separated. In this case the system is confined. For $\langle L \rangle \neq 0$ the quarks are screened and can be separated. The symmetry which is spontaneously broken is the center symmetry and will be discussed in section 3.5. This is only valid for pure gauge theory. For finite quark masses this is not fulfilled due to color charge screening through pair production.

3.3 Effective gauge theory

The full lattice formulation of QCD still suffers from some issues which makes it impossible to evaluate it in certain regimes. One is the sign problem at finite chemical potential. To get a better understanding of QCD, it is justified to make assumptions and study the theory in these limits. The assumptions made to derive the effective theory used in this work are the strong coupling limit ($\beta \to 0$) and the heavy quark limit ($\kappa \to 0$). For further details of the derivation of the effective theory we refer you to [4, 5].
First we shortly discuss the derivation of the Yang-Mills part of the effective action and how to formulate it in terms of Polyakov loops. Then we will investigate the hopping parameter expansion for heavy quarks.
The main idea of the effective theory is to simplify the path integral so that it only depends on temporal link variables. Therefore, a strong coupling expansion and a hopping parameter expansion is performed. Then we integrate over the spatial links.
We can rewrite equation 3.18 in the following way:

$$Z = \int [dU_0]\ e^{-S_{\text{eff}}}, \quad -S_{\text{eff}} = \ln \int [dU_i] \prod_f \det[Q_f] e^{-S_g} \tag{3.22}$$

For SU(3) it is possible to transform the integration measure over temporal gauge links into an integral over Polyakov loops L ($[dU_0] \to [dL]$). The Polyakov loop is given as:

$$L(\vec{x}) = \text{tr} \left[\prod_{t=0}^{N_\tau - 1} U_0(\vec{x}, t) \right] \tag{3.23}$$

Following the derivation in [6] we can rewrite the gauge action shown in equation 3.12 in terms of a character series. This is a sum over irreducible representations with the character χ and the dimension d.

$$-S_g[U] = \ln \prod_p [1 + \sum_{r \neq 0} d_r a_r(\beta) \chi_r(U_p)] + const \tag{3.24}$$

The character is the trace of the element in this representation. $\chi_r(U) = \text{tr}\ U^r$. Terms that do not contain temporal links are contained in a constant term and can be neglected since they factor out and can be absorbed in the partition function. So they do not influence expectation values. When neglecting plaquettes which do not contain any temporal links one obtains the leading order and ends up with a nearest neighbor interaction of Polyakov loops. It is important to mention that for SU(3) there is a fundamental and an anti-fundamental representation. Both have to be considered.

$$S^g_{\text{eff}} = -\sum_{\langle ij \rangle} \ln[1 + \lambda(\beta)(L_i L_j^* + L_i^* L_j)] \tag{3.25}$$

λ is now the effective gauge coupling parameter of the theory and depends on the inverse coupling β. It has been calculated to a high order [6]. In leading order λ is given as

$$\begin{aligned} \lambda &\approx u^{N_\tau} \\ u(\beta) &\approx \frac{\beta}{18} + \mathcal{O}(\beta^2), \end{aligned} \tag{3.26}$$

where u is the fundamental character expansion coefficient. Notice that this action contains only nearest neighbor interactions of Polyakov loops. One can see that the resulting theory is dimensionally reduced. This makes the numerical evaluation as well as the analytic treatment much easier.

3.4 Hopping parameter expansion

Besides the gauge action, we need an effective theory for the fermionic contributions [4]. We start with the hopping parameter representation of the Dirac operator introduced in equation 3.15. One uses the fact that the hopping parameter κ is small in the limit of large quark masses. This makes it possible to expand the quark determinant in the infinitely heavy quark regime. One can rewrite the determinant in the following way:

$$\det Q = \det[1 - T - S] = \det \underbrace{[1 - T]}_{Q_{\text{stat}}} \det \underbrace{\left[1 - \frac{1}{1-T}(S^+ + S^-)\right]}_{Q_{\text{kin}}}. \tag{3.27}$$

T are the hops in positive and negative temporal direction, S in spatial direction. The static determinant is obtained by considering only temporal hops. After calculating the spin and space contributions we end up with the following expression:

$$\begin{aligned} \det Q_{\text{stat}} &= \det \left[1 - \kappa e^{a\mu}(1+\gamma_0)U_0(x)\delta_{x,y-\hat{e}_0} - \kappa e^{-a\mu}(1-\gamma_0)U_0^\dagger(x-\hat{e}_0)\delta_{x,y+e_0}\right] \\ &= \prod_x \det\left[1 + (2\kappa e^{a\mu})^{N_\tau} W(x)\right]^2 \det\left[1 + (2\kappa e^{-a\mu})^{N_\tau} W^\dagger(x)\right]^2. \end{aligned} \tag{3.28}$$

From here it is possible to reformulate the Wilson lines $W(x)$ in terms of Polyakov loops.

$$\det Q_{\text{stat}} = \prod_x \left[1 + hL(x) + h^2 L^*(x) + h^3\right]^2 \left[1 + \overline{h}L^*(x) + \overline{h}^2 L(x) + \overline{h}^3\right]^2 \tag{3.29}$$

h and $\overline{h}$ are the effective quark and anti-quark couplings. They are given as:

$$\begin{aligned} h &= \exp(N_\tau(a\mu + \ln(2\kappa))) \\ \overline{h} &= \exp(N_\tau(-a\mu + \ln(2\kappa))), \end{aligned} \tag{3.30}$$

with the lattice spacing a, the chemical potential μ, and the hopping parameter κ. Furthermore it is possible to consider higher orders in the hopping parameter expansion.

Therefore, we consider the kinetic part of the determinant. It can be written in the following way:

$$\det Q_{\text{kin}} = \det[1 - P - M] = \exp\left[\text{tr}[\ln(1 - P - M)]\right]. \tag{3.31}$$

The logarithm has to be expanded and one ends up with traces of combinations of M and P matrices. They can be evaluated. A detailed calculation up to $\mathcal{O}(\kappa^4)$ is shown in [7]. The result for the two-point interaction of order κ^2 is given as:

$$\begin{aligned} -S^{\text{eff}}_{\kappa^2} = -2h_2 \sum_{x,i=1}^{3} \Bigg[\Bigg(\text{tr}\frac{hW(x)}{1+hW(x)} - \text{tr}\frac{\overline{h}W^\dagger(x)}{1+\overline{h}W^\dagger(x)} \Bigg) \\ \times \Bigg(\text{tr}\frac{hW(x+i)}{1+hW(x+i)} - \text{tr}\frac{\overline{h}W^\dagger(x+i)}{1+\overline{h}W^\dagger(x+i)} \Bigg) \Bigg]. \end{aligned} \tag{3.32}$$

h_2 is the nearest neighbor interaction strength and is given as $h_2 = \frac{\kappa^2 N_\tau}{3}$.
The κ^4 corrections can also be evaluated. Since we use them only in the heavy dense limit ($\overline{h} \to 0$) we show only these terms. The full expression for the kinetic determinant up to κ^4 can be found in the appendix of [7]. A detailed derivation of the κ^2 and κ^4 terms is also found there. The κ^4 contributions in the heavy dense case yield

$$\begin{aligned} -S^{\text{eff}}_{\kappa^4} = 2h_2^2 \sum_{x,i=1}^{3} \text{tr}\frac{hW(x)}{(1+hW(x))^2} \, \text{tr}\frac{hW(x+i)}{(1+hW(x+i))^2} \\ + \; h_2^2 \sum_{\substack{x,i=1,\\ j=1}}^{3} \text{tr}\frac{hW(x)}{(1+hW(x))^2} \, \text{tr}\frac{hW(x-i)}{1+hW(x-i)} \, \text{tr}\frac{hW(x-j)}{1+hW(x-j)} \\ +2h_2^2 \sum_{\substack{x,i=1,\\ j=1}}^{3} \text{tr}\frac{hW(x)}{(1+hW(x))^2} \, \text{tr}\frac{hW(x-i)}{1+hW(x-i)} \, \text{tr}\frac{hW(x+j)}{1+hW(x+j)} \\ + \; h_2^2 \sum_{\substack{x,i=1,\\ j=1}}^{3} \text{tr}\frac{hW(x)}{(1+hW(x))^2} \, \text{tr}\frac{hW(x+i)}{1+hW(x+i)} \, \text{tr}\frac{hW(x+j)}{1+hW(x+j)}. \end{aligned} \tag{3.33}$$

The traces over fractions of temporal Wilson lines can be expressed in terms of Polyakov loops. This is shown in appendix A.2. The partition function for one flavor up to order κ^4 in the heavy dense case is then given as

$$Z = \int [dL] \; \det Q_{\text{stat}} \; e^{-(S_g^{\text{eff}} + S_{\kappa^2}^{\text{eff}} + S_{\kappa^4}^{\text{eff}})} + \mathcal{O}(\kappa^6). \tag{3.34}$$

3.5 Center symmetry

As we mentioned before, phase transitions are closely related to the symmetry breaking. The deconfinement transition in the heavy quark limit is associated with center symmetry. It is a topologically non-trivial gauge symmetry which is realized only at

finite temperature. Due to the temporal boundary conditions, the gauge links can be transformed in the the following way:

$$U_0(x, t_0) \to h\ U_0(x, t_0 + \frac{1}{aN_\tau}). \tag{3.35}$$

The action is invariant under such a transformation if $h \in Z(3)$. This is called the center of $SU(3)$ and contains the cubic roots $(1,\ e^{\frac{2\pi i}{3}},\ e^{\frac{4\pi i}{3}})$. Since the gauge action consists of gauge links, it is invariant under such transformations. Hence, center symmetry is realized for all gauge invariant objects which are closed in a trivial way in the temporal direction. This is not the case for the Polyakov loop L since it winds through the whole time direction on the lattice and is only closed in a non-trivial way. Consequently, it is not invariant under center symmetry but transforms as

$$L \to h\ L. \tag{3.36}$$

Center symmetry is spontaneously broken if the expectation value of the Polyakov loop is non-zero and restored otherwise. At low temperatures the color charges are confined. At high temperatures the symmetry breaks since one sector of the center symmetry is favored. This corresponds to the deconfinement phase. This explains why the Polyakov loop is an order parameter for center symmetry.
However, this is not true for fermions. They break center symmetry explicitly due to their anti-periodic boundary conditions in temporal direction. This leads to a non-vanishing Polyakov loop in the low temperature phase. It can be interpreted as the color charge screening through pair production.

3.6 QCD phase diagram

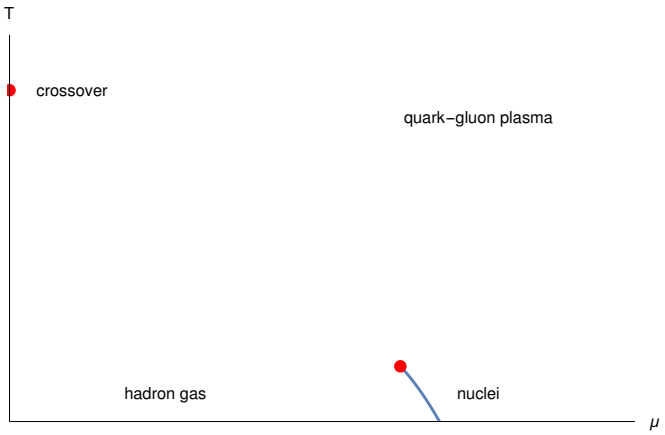

(a) Qualitative QCD phase diagram from the theoretical and experimental perspective.

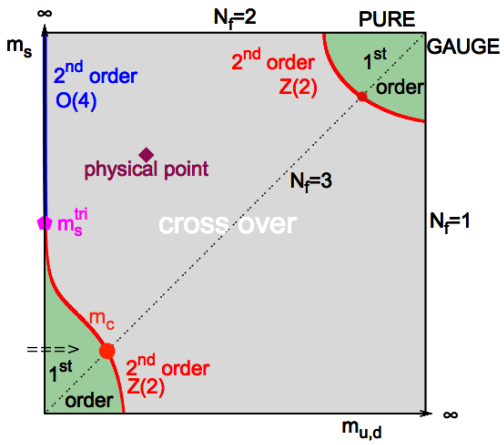

(b) Columbia plot [8]

QCD has thermodynamic properties and can be visualized in a phase diagram. It describes strong interacting matter in equilibrium. The phase diagram is still largely unknown from first principles and experiments. The properties of the QCD phase diagram which are confirmed are visualized in figure 3a. From lattice calculations

we know that the transition between hadronic matter and the quark-gluon plasma at vanishing chemical potential is a crossover. This is due to two different aspects of the transition which are confinement and chiral symmetry. Chiral symmetry is fulfilled for massless quarks, center symmetry for infinitely heavy quarks. Both are explicitly broken under physical conditions (physical point). The phase diagram at zero chemical potential is very well known from first principle calculations and can be visualized in the Columbia plot (Figure 3b). It shows the transition at $\mu = 0$ depending on the quark masses. The x axis scales the mass of the up and down quark, the y axis the mass of the strange quark. Up and down can be plotted on the same axis since their masses are very similar. The phase transition for different number of flavors can be studied. The different numbers of flavors are relevant since the quark's dynamic can be neglected in the heavy quark limit and they decouple from the theory in this region. As one can see the transition strongly depends on the masses of the quarks. For light quarks the transition is of first order and the associated symmetry is chiral symmetry. The order parameter is the chiral condensate. It ends in a second order critical line. For very heavy quarks the transition is again of first order but the corresponding symmetry is center symmetry. This is the deconfinement transition. The effective Polyakov theory is valid in this region. The physical point is located between these two regions where the transition is a crossover.
The finite μ region is not accessible for lattice QCD due to the sign problem. A unknown question is, if the transition between hadronic matter and the quark-gluon plasma turns into a real phase transition at high densities. This would indicate a critical point. There are several effective models which predict a phase transition but so far the existence of a critical endpoint remains unknown. Most of these theories which often rely on phenomenological assumptions can only describe certain parameter regions of the phase diagram.
Another property of QCD is the liquid-gas transition of nuclear matter. At low values of μ strong interacting matter is a hadron gas while at a certain point nuclear matter forms nuclei. This transition is of first order and end in a critical point for higher temperatures.

4 The mean field analysis

4.1 Pure gauge theory

As shown in the previous section the lattice gauge action of QCD can be expressed in terms of a nearest neighbor Polyakov loop interaction in the strong coupling expansion. In this section we want to apply a mean field method to the effective theory to get an analytical insight into the physics of the effective theory. Mean field theory will lead to a factorization of the partition function. This turns the integrand in a product over Polyakov loops which can be evaluated analytically. As we will see this keeps a lot of the properties of the full theory although strong fluctuations are neglected. The starting point is the gauge action.

$$\exp(-S_{\text{eff}}) = \prod_{\langle ij \rangle} [1 + \lambda(L_i^* L_j + L_i L_j^*)] \tag{4.1}$$

The L_i are Polyakov loops which can be seen as spins. They are traces over temporal Wilson lines and can be treated as complex numbers. The product is over nearest neighbors. Notice that the action is logarithmic. The expectation value for an observable is then given as

$$\begin{aligned} \langle \mathcal{O}(L) \rangle =& \frac{1}{Z_0} \int [dL] \left[\mathcal{O}(L) e^{-S_{\text{eff}}} \right] \\ Z_0 =& \int [dL] \left[e^{-S_{\text{eff}}} \right]. \end{aligned} \tag{4.2}$$

Since all links L_i are coupled to their nearest neighbors it is not possible to solve these integrals analytically. To get a better insight into this effective theory one has to come up with an ansatz to decouple the Polyakov loops so that the path integral factorizes. Therefore, we rewrite the action in the following form where the product over next neighbors turns into a sum.

$$-S_{\text{eff}} = \sum_{\langle ij \rangle} \ln[1 + \lambda(L_i^* L_j + L_i L_j^*)] \tag{4.3}$$

Next, we rewrite the logarithm in its series form. Note, that the Mercator series is only convergent for $|\lambda(L_i L_j^* + L_i^* L_j)| < 1$. Since we know that L is an order parameter in pure gauge theory and it is zero in the disordered phase this should be sufficient.

$$-S_{\text{eff}} = \sum_{\langle ij \rangle} \sum_{k=1}^{\infty} \frac{(-1)^{k+1}}{k} (\lambda(L_i L_j^* + L_i^* L_j))^k \tag{4.4}$$

From here, we introduce a mean field ansatz $L_i = \bar{L} + \delta L_i$ and neglect all higher powers in the fluctuations so that the spins decouple. This is done because in mean field theory we only consider linear fluctuations so that the free energy of the single-sites are additive.

$$(L_i L_j^* + L_i^* L_j) = 2|\bar{L}|^2 + \underbrace{\bar{L}^*(\delta L_i + \delta L_j) + \bar{L}(\delta L_i^* + \delta L_j^*)}_{=B_i + B_j} + \mathcal{O}(\delta L^2) \tag{4.5}$$

Inserting the ansatz into the action we can reformulate it as

$$\begin{aligned} -S_{\text{eff}} &= \sum_{\langle ij \rangle} \sum_{k} \frac{(-1)^{k+1}}{k} (A + B_i + B_j)^k + \mathcal{O}(\delta L^2) \\ &\approx \sum_{\langle ij \rangle} \sum_{k} \frac{(-1)^{k+1}}{k} (A^k + kA^{k-1}(B_i + B_j)) \end{aligned} \tag{4.6}$$

Where $A = 2\lambda|\bar{L}|^2$ and $B_i = \lambda(\bar{L}(\delta L_i^*) + \bar{L}^*(\delta L_i))$.
Since the sum over next neighbors is finite and we assumed $|\lambda(L_i L_j^* + L_i^* L_j)| < 1$ so that the Mercator series converges absolutely we can exchange the sums and are able to simplify the sum over next neighbors. Therefore, we look at the last term in the previous expression.

$$\sum_{\langle ij \rangle} (A + k(B_i + B_j)) = \sum_{x,i=1}^{3} \left(2|\bar{L}|^2 + k(\bar{L}\delta L_x^* + \bar{L}^* \delta L_x + \bar{L}\delta L_{x+i}^* + \bar{L}^* \delta L_{x+i}) \right) \tag{4.7}$$

Now, we can split up the sums and relabel the indices $x + i \to x$. This can be done because of periodic boundary conditions in spatial direction. Since this has to be done in all spatial directions one picks up a factor of d for the number of spatial dimensions.

$$\begin{aligned} &\sum_{x} \sum_{i=1}^{3} \left[|\bar{L}|^2 + k\bar{L}\delta L_x^* + k\bar{L}^* \delta L_x + |\bar{L}|^2 + k\bar{L}\delta L_{x+i}^* + k\bar{L}^* \delta L_{x+i} \right] \\ =& 2d \sum_{x} \left[|\bar{L}|^2 + k(\bar{L}\delta L_x^* + \bar{L}^* \delta L_x) \right] \end{aligned} \tag{4.8}$$

Note that we only summed over neighbors in positive spatial direction to avoid double counting. Now we re-substitute the $\delta L_i = L_i - \bar{L}$ which leads us to the following expression.

$$\begin{aligned} -S_{\text{eff}} = 2d\lambda \sum_{k=1}^{\infty} \frac{(-1)^{k+1}}{k} (2\lambda|\bar{L}|^2)^{k-1} \sum_{x} \left((1-2k)|\bar{L}|^2 + k(\bar{L}L_x^* + \bar{L}^* L_x) \right) \\ + \mathcal{O}(\delta L^2) \end{aligned} \tag{4.9}$$

For the next step we compute the sum over k which is still true for the convergent region of the Mercator series. From here on we will neglect higher orders.

$$-S_{\text{eff}} \approx d \sum_{x} \left[\ln[1 + 2\lambda|\bar{L}|^2] + \frac{4\lambda|\bar{L}|^2}{1 + 2\lambda|\bar{L}|^2} + \frac{2\lambda}{1 + 2\lambda|\bar{L}|^2} (\bar{L}L_x^* + \bar{L}^* L_x) \right] \tag{4.10}$$

Since the first two terms are independent of L_x we are able to factor them out in the partition function and we can write equation 4.2 as

$$Z_0 = \mathcal{C} \int [dL] \exp \left\{ \sum_{x} \underbrace{\frac{2d\lambda}{1 + 2\lambda|\bar{L}|^2} (\bar{L}L_x^* + \bar{L}^* L_x)}_{-S_{\text{ss}}} \right\} \tag{4.11}$$

Now, it is clear to see that also the partition function over the different lattice sites factorizes.
From statistical physics the relation between the free energy F and the partition function is given as:

$$Z_0 = e^{-F} = \mathcal{C} \int [dL] e^{-\sum_x S_{\text{ss}}} = \mathcal{C} \prod_x \underbrace{\int dL \; e^{-S_{\text{ss}}}}_{Z_{\text{ss}}:=} = \mathcal{C} \prod_x e^{-F_{\text{ss}}} \tag{4.12}$$

This relation shows that the total free energy F can be computed by adding the free energy of each lattice site F_{ss}. If we take the logarithm of the previous equation one can see that the following holds:

$$-\sum_x F_{\text{ss}} = \sum_x \ln Z_{\text{ss}} \tag{4.13}$$

Note that the constant $\mathcal{C}$ only shifts the whole free energy by a constant value $\ln \mathcal{C}$. Since in physics we just measure energy differences this constant is irrelevant and can be neglected. Since all lattice sites contribute equally and are independent from each other we can just deal with the single-site free energy. It can be interpreted as free energy density because the sum over all lattice sites contributes a factor of N_s^3 which is the volume of the system.

$$F_{\text{ss}} = -\ln(Z_{\text{ss}}) = -\ln \left[\int dL \; \exp \left\{ \frac{2d\lambda}{1 + 2\lambda |\bar{L}|^2} (\bar{L} L^* + \bar{L}^* L) \right\} \right] \tag{4.14}$$

The equilibrium state is given by the minimum of the free energy F. If we take the derivative of F_{ss} with respect to the mean value $\bar{L}^*$ we get the following expression:

$$\frac{\partial F_{\text{ss}}}{\partial \bar{L}^*} = -\frac{2d\lambda}{1 + 2\lambda |\bar{L}|^2} \langle L \rangle_{\text{ss}} + \frac{4d\lambda^2 \bar{L}}{(1 + 2\lambda |\bar{L}|^2)^2} \left(\bar{L} \langle L^* \rangle_{\text{ss}} + \bar{L}^* \langle L \rangle_{\text{ss}} \right) \tag{4.15}$$

The expectation values of L and L^* are now computed similarly as in equation 4.2 and we claim them to be identical with the mean values of the Polyakov loops we introduced in the mean-field ansatz $\bar{L}$. This is called self-consistency equation. This assumption is justified due to the fact that no Polyakov loop is unique and its expectation value should be the same as the mean field value of the surrounding spins.

$$\begin{aligned} \bar{L} &\stackrel{!}{=} \langle L \rangle_{\text{ss}} = \frac{1}{Z_{\text{ss}}} \int dL \left\{ L \; \exp \left(\frac{2d\lambda}{1 + 2\lambda |\bar{L}|^2} (\bar{L} L^* + \bar{L}^* L) \right) \right\} \\ \bar{L}^* &\stackrel{!}{=} \langle L^* \rangle_{\text{ss}} = \frac{1}{Z_{\text{ss}}} \int dL \left\{ L^* \; \exp \left(\frac{2d\lambda}{1 + 2\lambda |\bar{L}|^2} (\bar{L} L^* + \bar{L}^* L) \right) \right\} \end{aligned} \tag{4.16}$$

Following the procedure done in [9] we introduce a mean field free energy F_{mf} which has to be minimized with respect to the order parameter. This is done to find the global minimum of the free energy F and indicates that non-trivial solutions for $\bar{L}$ can be found by minimizing F_{mf}.

$$F_{\text{mf}} = F_{\text{ss}}(\lambda) + \overline{F}(\lambda, \bar{L}, \bar{L}^*) \tag{4.17}$$

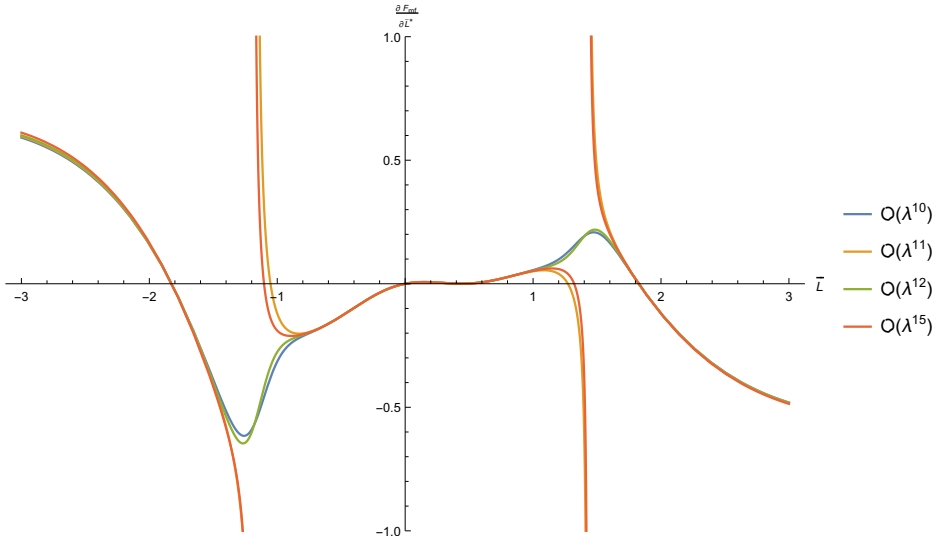

Figure 4: The change in the mean-field free energy expanded for different orders in λ at $\lambda = 0.15$. The agreement between the plots is good for $|\bar{L}| < 1$. In this region the required condition for the absolute convergence of the Mercator series $2\lambda|\bar{L}|^2 < 1$ is fulfilled.

$$0 \stackrel{!}{=} \frac{1}{2d\lambda}\frac{\partial F_{\mathrm{mf}}}{\partial \bar{L}^*} = -\frac{\langle L\rangle_{\mathrm{ss}}}{1+2\lambda|\bar{L}|^2} + \frac{2\lambda\bar{L}}{(1+2\lambda|\bar{L}|^2)^2}(\bar{L}\langle L^*\rangle_{\mathrm{ss}} + \bar{L}^*\langle L\rangle_{\mathrm{ss}}) + \frac{1}{2d\lambda}\frac{\partial \overline{F}}{\partial \bar{L}^*} \tag{4.18}$$

Using the self-consistent condition from equation 4.16 we find the following differential equation.

$$\frac{1}{2d\lambda}\frac{\partial \overline{F}}{\partial \bar{L}^*} = \frac{\bar{L}}{1+2\lambda|\bar{L}|^2} - \frac{4\lambda\bar{L}|\bar{L}|^2}{(1+2\lambda|\bar{L}|^2)^2} \tag{4.19}$$

$\overline{F}$ only depends on the mean fields $\bar{L}$ and $\bar{L}^*$. This differential equation can be solved analytically and we get

$$\overline{F}(\bar{L},\bar{L}^*) = 2d\left[\frac{1}{1+2\lambda|\bar{L}|^2} + \frac{3}{2}\ln(1+2\lambda|\bar{L}|^2)\right] + c \tag{4.20}$$

As we pointed out the constant c is irrelevant and can be absorbed into the free energy but we choose it in a way that the minimum of $\mathcal{F}_{\mathrm{mf}}$ at $|\bar{L}| = 0$ is at zero. The derivative of $\overline{F}$ with respect to $\bar{L}^*$ contributes the last two terms in equation 4.18.
At this point it is worth mentioning the similarity between the mean field free energy from our theory (equation 4.17) and Landau's description of the free energy (equation 2.5). The free energy F_{mf} is also a function only depending on the two component order parameter $\bar{L}$ and $\bar{L}^*$ and the effective coupling λ from the gauge theory.
To compute the single-site free energy F_{mf} integrals over Polyakov loops have to be evaluated. We point out the procedure in the appendix A.1.

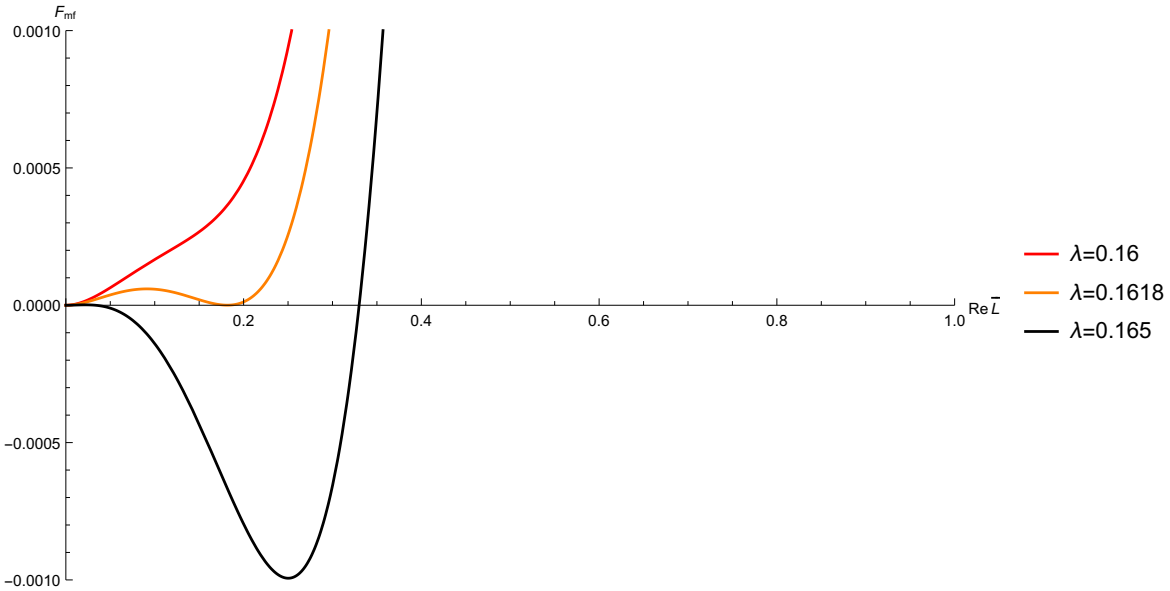

Figure 5: The mean-field free energy around the phase transition

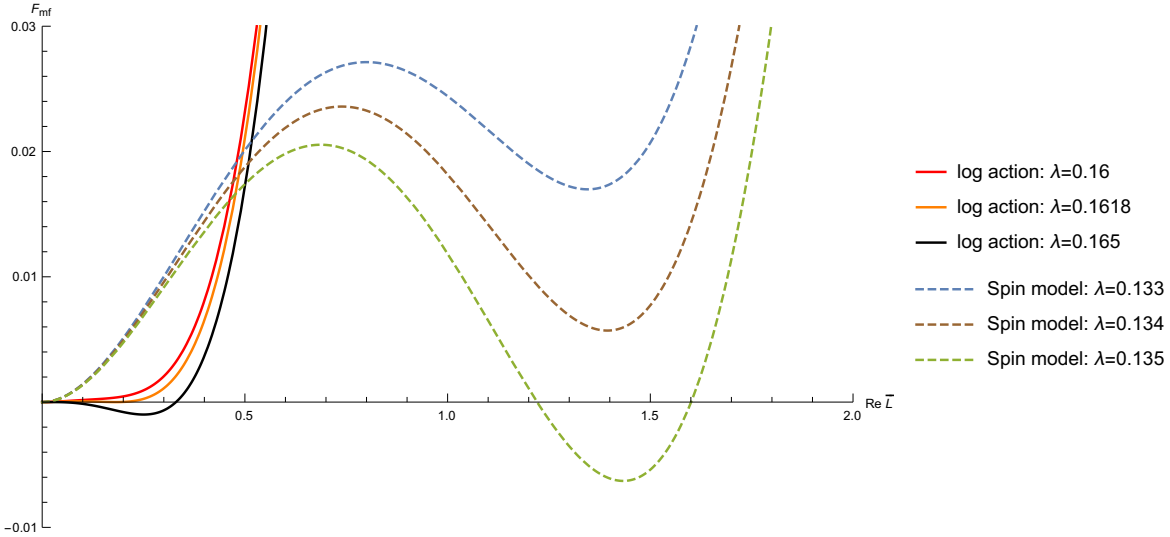

Figure 6: The mean field free energy $\mathcal{F}_{\text{mf}}$ for SU(3) for different values of λ compared with the mean field free energy of the spin model action from [10].

To calculate F_{ss} we have to expand the exponential in equation 4.14. To check for convergence we expand up to different orders and compare the results for the mean field free energy. As one can see in figure 4 the convergence is reliable for $|\text{Re}\bar{L}| < 1$. This corresponds to the convergence region of the Mercator series used in the derivation of the mean field gauge action. The convergence radius can be roughly estimated as $|\bar{L}| < \sqrt{1/(2\lambda)}$.
Now, we reached the point to search for a phase transition in the gauge theory. Therefore, the mean field free energy (equation 4.17) is plotted on $\text{Re}\bar{L}$. The result is plotted in figure 5 for different values of λ. As one can see, the global minimum is located in the origin. This corresponds to the disordered phase where the order parameter $\bar{L}$ is

zero and the theory is confined. Although the expectation value of the Polyakov loop $\bar{L}$ is in general complex it is sufficient to plot only its positive real part. Due to center symmetry this corresponds to one of the Polyakov loop sectors.
When we increase λ which corresponds to increasing the temperature the global minimum gets degenerated. According to Landau theory this implies a first-order phase-transition. At this point the order parameter $\bar{L}$ "jumps" to a non-zero value. This transition occurs at:

$$\lambda_{\text{crit}} = 0.1618 \tag{4.21}$$

This means that the phase transition in pure gauge theory between the confined and deconfined phase is of first order. If we compared it with the numerical results in [6] ($\lambda_{\text{crit}} = 0.187885$) the deviation is 14%. This is in agreement with the expectations from mean field theory. This analysis show qualitatively the same behavior as the spin model [10] although it is quantitatively better compared to [6]. One reason for this is that the spin action is a more inaccurate approximation of the logarithm effective action since it corresponds only to the leading term in the logarithmic expansion ($k = 1$ in equation 4.4). There, the phase transition occurs at $\lambda_{\text{crit}} = 0.134$.

4.2 Static quark determinant

We have to consider the quark determinant $\det Q$ introduced in equation 3.27 to include fermions into the analysis. The partition function then reads

$$Z_0 = \int [dL] \prod_{f=1}^{N_f} \det Q \; e^{-S_{\text{eff}}}. \tag{4.22}$$

We will limit the analysis to one flavor but it is possible to extend it to an arbitrary number of flavors. For convenience we start with the simplest case. Therefore, only the static determinant is considered. In this case $\det Q_{\text{kin}} = 1$. This corresponds to infinitely heavy quarks and only hops in temporal direction are included. The traces over temporal Wilson lines can be expressed in Polyakov loops and the determinant yields

$$\det Q_{\text{stat}} = \exp(-S_0) = \prod_i \left(1 + hL_i + h^2 L_i^* + h^3\right)^2 \left(1 + \overline{h} L_i^* + \overline{h}^2 L_i + \overline{h}^3\right)^2. \tag{4.23}$$

Since the static determinant does not couple neighboring Polyakov loops the partition function factorizes as in equation 4.12 and it is sufficient to deal with the single-site quark determinant. In expanded form it is given as

$$\begin{aligned} f(L, L^*, h, \overline{h}) = (\det Q_{\text{stat}})_{\text{ss}} = \gamma_1 + \gamma_2 L^* + \gamma_3 L + \gamma_4 L^{*2} + \gamma_5 L^2 + \gamma_6 L L^* \\ + \gamma_7 L L^{*2} + \gamma_8 L^* L^2 + \gamma_9 L^{*3} + \gamma_{10} L^3 + \gamma_{11} L^2 L^{*2} \\ + \gamma_{12} L L^{*3} + \gamma_{13} L^3 L^* + \gamma_{14} L^4 + \gamma_{15} L^{*4}. \end{aligned} \tag{4.24}$$

The coefficients are given in table 1. As a remark one should notice that the fermionic contributions break the center symmetry explicitly. Unlike the Yang-Mills part from section 4.1 where the symmetry is spontaneously broken the fermionic part leads to a

non-zero order parameter in the confined phase.

$$
\begin{aligned}
\gamma_1 &= \alpha_1(h)\alpha_1(\overline{h}) && \alpha_1(x) = (1+x^3)^2 \\
\gamma_2 &= \alpha_1(h)\alpha_2(\overline{h}) + \alpha_3(h)\alpha_1(\overline{h}) && \alpha_2(x) = 2(x+x^4) \\
\gamma_3 &= \alpha_1(h)\alpha_3(\overline{h}) + \alpha_2(h)\alpha_1(\overline{h}) && \alpha_3(x) = 2(x^2+x^5) \\
\gamma_4 &= \alpha_1(h)\alpha_4(\overline{h}) + \alpha_3(h)\alpha_2(\overline{h}) + \alpha_5(h)\alpha_1(\overline{h}) && \alpha_4(x) = x^2 \\
\gamma_5 &= \alpha_1(h)\alpha_5(\overline{h}) + \alpha_2(h)\alpha_3(\overline{h}) + \alpha_4(h)\alpha_1(\overline{h}) && \alpha_5(x) = x^4 \\
\gamma_6 &= \alpha_1(h)\alpha_6(\overline{h}) + \alpha_2(h)\alpha_2(\overline{h}) + \alpha_3(h)\alpha_3(\overline{h}) + \alpha_6(h)\alpha_1(\overline{h}) && \alpha_6(x) = 2x^3 \\
\gamma_7 &= \alpha_2(h)\alpha_4(\overline{h}) + \alpha_3(h)\alpha_6(\overline{h}) + \alpha_5(h)\alpha_3(\overline{h}) + \alpha_6(h)\alpha_2(\overline{h}) \\
\gamma_8 &= \alpha_2(h)\alpha_6(\overline{h}) + \alpha_3(h)\alpha_5(\overline{h}) + \alpha_4(h)\alpha_2(\overline{h}) + \alpha_6(h)\alpha_3(\overline{h}) \\
\gamma_9 &= \alpha_3(h)\alpha_4(\overline{h}) + \alpha_5(h)\alpha_2(\overline{h}) \\
\gamma_{10} &= \alpha_2(h)\alpha_5(\overline{h}) + \alpha_4(h)\alpha_3(\overline{h}) \\
\gamma_{11} &= \alpha_4(h)\alpha_4(\overline{h}) + \alpha_5(h)\alpha_5(\overline{h}) + \alpha_6(h)\alpha_6(\overline{h}) \\
\gamma_{12} &= \alpha_5(h)\alpha_6(\overline{h}) + \alpha_6(h)\alpha_4(\overline{h}) \\
\gamma_{13} &= \alpha_4(h)\alpha_6(\overline{h}) + \alpha_6(h)\alpha_5(\overline{h}) \\
\gamma_{14} &= \alpha_4(h)\alpha_5(\overline{h}) \\
\gamma_{15} &= \alpha_5(h)\alpha_4(\overline{h})
\end{aligned}
$$

Table 1: Coefficients for the single-site static quark determinant.

The single-site partition function with static quarks is then given as

$$Z_{\mathrm{ss}}^{(\mathrm{q})} = \int dL \; f(L, L^*, h, \overline{h}) \; e^{-S_{\mathrm{ss}}} \tag{4.25}$$

We used the pure gauge single-site action (equation 4.11). The mean field free energy is then computed as in equation 4.17 but with the adjusted single-site free-energy. $\overline{F}$ stays unchanged because the static determinant is independent of the mean field $\overline{L}^*$. Thus, static quarks shift the free energy only by a constant factor which cannot be observed in a measurement. The derivative $\partial(\log(\int [dU_0] f(L, L^*, h, \overline{h})))/\partial \overline{L}^* = 0$ and we do not get any contributions to change $\overline{F}$ (equation 4.20). So, the mean field free energy is:

$$F_{\mathrm{mf}} = -\ln(Z_{\mathrm{ss}}^{(\mathrm{q})}) + \overline{F} \tag{4.26}$$

To understand the effects of static quarks we start with the case where the chemical potential μ is zero. In this case $h = \overline{h}$ and the theory has two free parameters h and λ. To understand the effects on the deconfinement phase transition from the previous section we slowly start to turn on the quark coupling h and observe what happens with the degeneracy of the global minimum of F_{mf}. This corresponds to increasing κ and N_τ. This corresponds to lowering the masses of the quarks.
The mean field free energy for different values of h at the phase transition is plotted in figure 7. One important observation is the explicit breaking of center symmetry. The minimum of the free energy, corresponding with the confined phase which is in the origin for vanishing quark coupling is shifted into the positive direction of the real part of the Polyakov loop. Moreover, the degeneracy of the minimum at the phase transition becomes smoothed out until it vanishes at $h_{\mathrm{crit}} = 0.00065$. At this point the

phase transition turns from first to second order. There, not only the first derivative of the mean field free energy is zero but also the second derivative. This is shown in figure 8. There the shift of the global minimum is not any longer discontinuous but turns continuously from one phase to the other. This point is called the critical endpoint. When further increasing h the transition turns into a crossover. The two phases are no longer separated by a strict boundary and can not be distinguished. The effective gauge coupling is also effected by the quark determinant. It gets smaller for rising quark coupling.
The observed results agree with previous works [10, 11]. They, for expample, found the critical endpoint $(h_{\text{crit}}, \lambda_{\text{crit}})$ to be at $h_{\text{crit}} = 0.000731$, $\lambda_{\text{crit}} = 0.18672$ [11]. This is a relative discrepancy of 11% in h_{crit} and 14% in λ_{crit}.
Finally we plot the phase boundary in the $h - \lambda$ plane (figure 9). As on can see the critical coupling between the confined and the deconfined phase shrinks until the critical endpoint is reached. At this point, the phase transition turns from first to second order. Increasing h further turns the transition into a crossover where the order parameter changes smoothly. This diagram corresponds to the upper right corner of figure 3b. At a certain point the Polyakov loop can no longer be used as an indicator for the phase transition. It is no longer an order parameter.
Now, we want to understand which parts of the effective coupling contribute the most to these effects. We observed that for vanishing chemical potential ($h = \overline{h}$) the critical endpoint appears at very small values of h. Therefore, it is reasonable to expand the static quark determinant (equation 4.24) around $h = 0$.

$$f(L, L^*, h) = 2h(L + L^*) + \mathcal{O}(h^2) \tag{4.27}$$

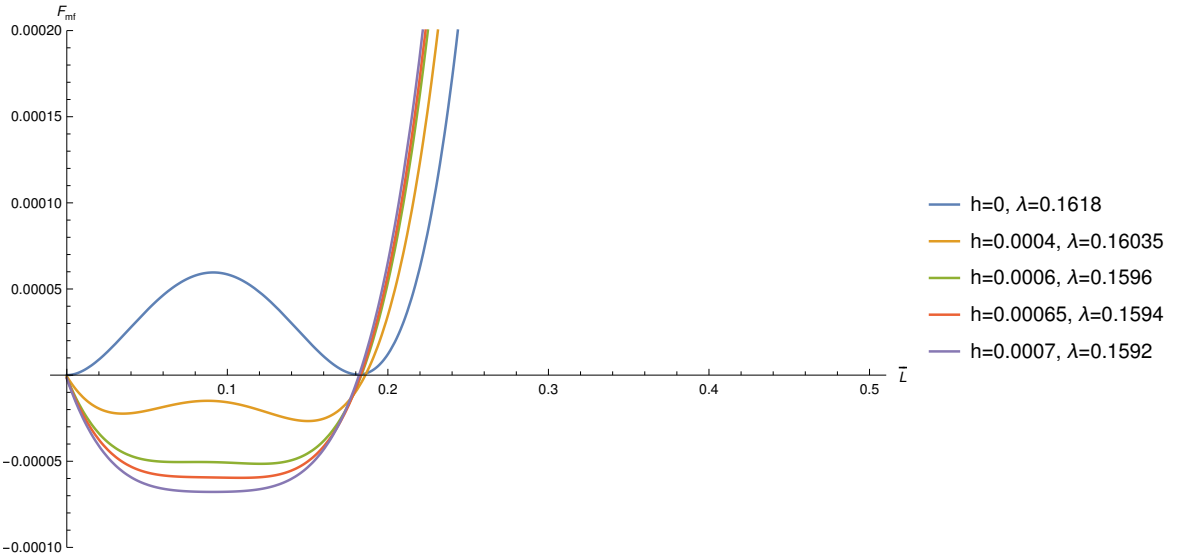

Figure 7: The change in the phase-transition for different values of h at zero baryon density.

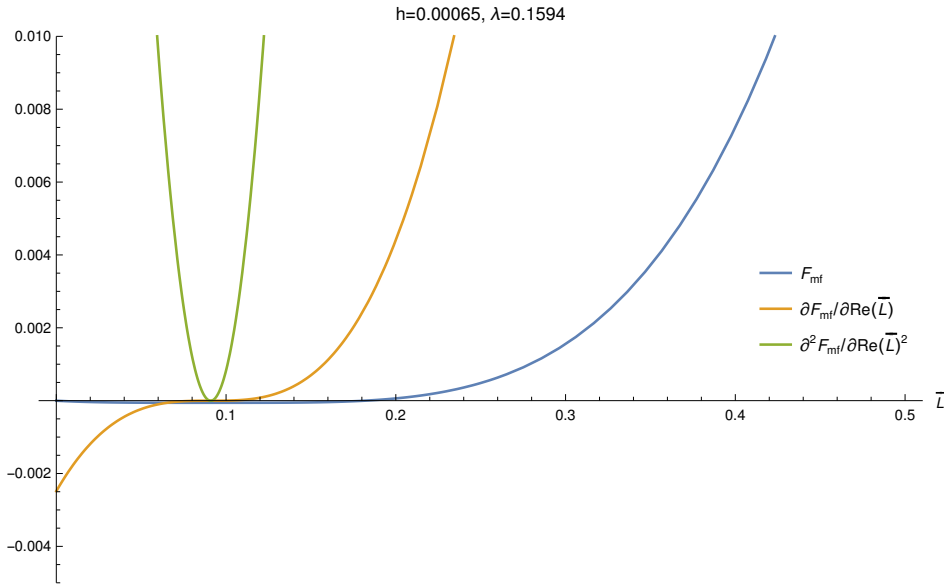

Figure 8: The mean field free energy and its derivatives at the critical endpoint. Both, the first and second derivative is zero. This is the critical end point where a second order phase transition occurs.

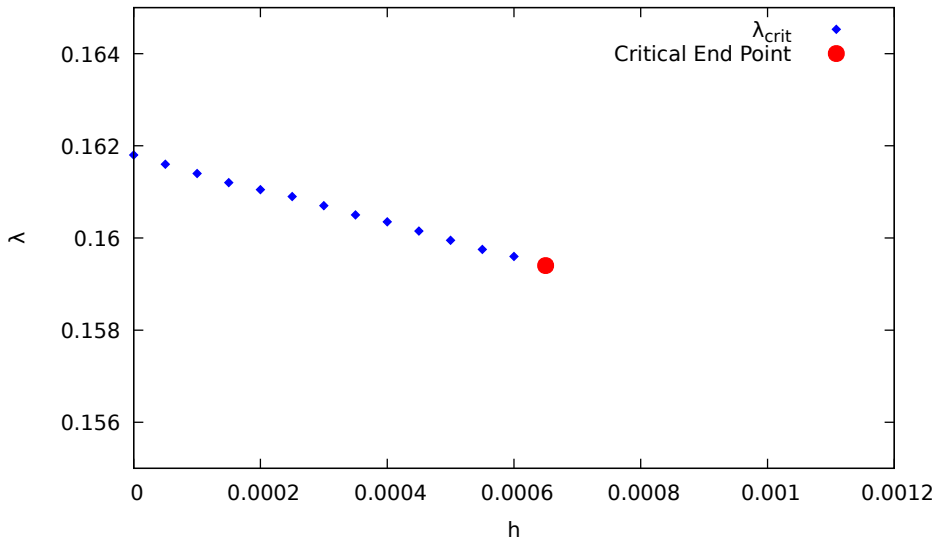

Figure 9: The phase boundary between the confinement and deconfinement phase. When turning on the effective quark coupling h the phase transition turns from first order to a continuous transition.

We discover that we get the same result (figure 10) as with the full static mean field determinant. Therefore the main contribution is only due to the leading terms in h. This is a consequence of the very small value for h_{cep}. The critical endpoint occurs at a magnitude of 10^{-4} .
This leads us to the conclusion that higher orders in the hopping parameter will not

affect the behavior of the deconfinement phase transition since their leading term is of higher order in h.
Nevertheless, it is worthwhile to study higher terms in a different parameter regime where h is not small which is the parameter region of the liquid-gas transition of nuclear matter. Thus, we will derive the mean field version of the kinetic quark determinant for $\mathcal{O}(\kappa^2)$ and $\mathcal{O}(\kappa^4)$ in the following sections.

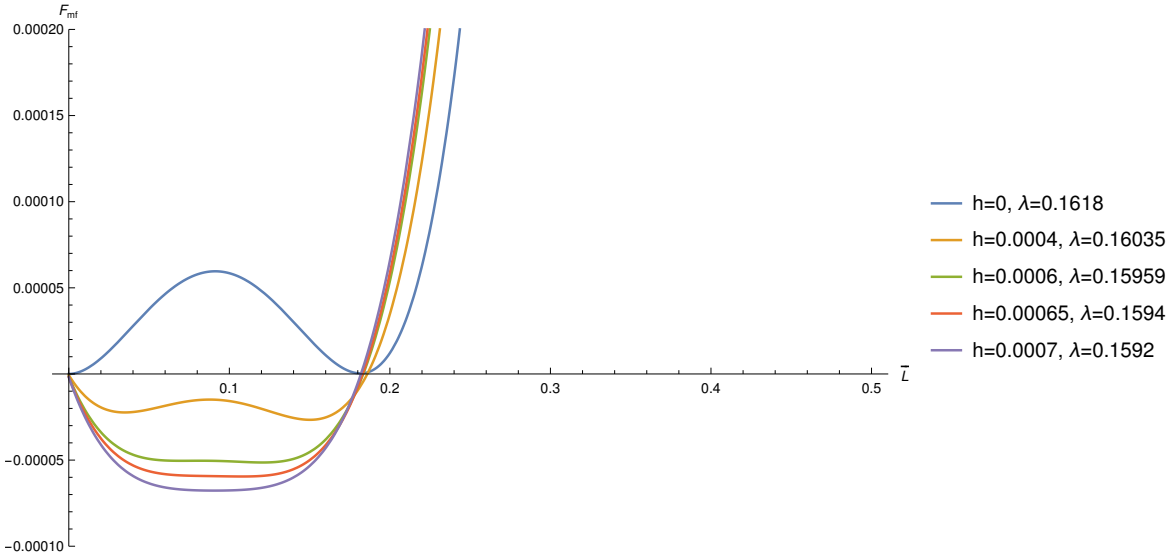

Figure 10: The change in the phase transition for different values of h with the static quark determinant expanded in h up to linear order.

5 Kinetic quark determinant

5.1 κ^2 corrections

Until now, we considered only the case where the quarks in the system were infinitely heavy. To investigate into the region of finite, although heavy quarks, one has to include spatial hops of the quark determinant (equation 3.27). These are kinetic terms of the quarks. We can write the fermionic contributions to the partition function as an expansion in κ:

$$S_{\text{eff}}^{\text{fer}} = S_0 + S_{\kappa^2}^{\text{eff}} + \mathcal{O}(\kappa^4) \tag{5.1}$$

The general expression of the κ^2 corrections for the heavy dense case ($\overline{h} \to 0$) is shown in equation 3.32. In appendix A.2 we show how to express the fractals of traces over Wilson lines in terms of Polyakov loops. Since we study the theory in the heavy dense region ($\overline{h} \to 0$) only the following terms survive

$$S_{\kappa^2}^{\text{eff}} = 2h_2 \sum_{x,i} [W_{1,0}(x) W_{1,0}(x+i)] \tag{5.2}$$

with

$$W_{1,0} = \text{tr} \frac{h\ W}{1 + h\ W}. \tag{5.3}$$

In terms of Polyakov loops this reads

$$W_{1,0}(x) = \frac{hL_x + 2h^2 L_x^* + 3h^3}{1 + hL_x + h^2 L_x^* + h^3}. \tag{5.4}$$

This expression can even be more simplified. Without any approximation one can proof that the highest power in h is of order $2N_cN_f$. Since we only work with three colors and 1 flavor it is sufficient to expand $W_{1,0}(x)$ up to $\mathcal{O}(h^6)$.

$$\begin{aligned} W_{1,0}(x) =& hL_x + (2L_x^* - L_x^2)h^2 + (3 + L_x^3 - 3L_xL_x^*)h^3 \\ &+ (4L_x^2L_x^* - 4L_x - L_x^4 - 2(L_x^*)^2)h^4 \\ &+ (5L_x^2 + L_x^5 - 5L_x^* - 5L_x^3L_x^* + 5L_x(L_x^*)^2)h^5 \\ &+ (12L_xL_x^* - 3 - 6L_x^3 - L_x^6 + 12L_xL_x^* + 6L_x^4L_x^* - 9L_x^2(L_x^*)^2 + 2(L_x^*)^3)h^6 \end{aligned} \tag{5.5}$$

From here, we are able to proceed similarly as for the gauge action. First the expanded expression is inserted into the action (equation 5.2). Then we replace the particular Polyakov loops and the complex conjugate by the mean field expression ($L_x = \bar{L} + \delta L_x$ and $L_x^* = \bar{L}^* + \delta L_x^*$) and expand them up to linear order.

$$
\begin{aligned}
W_{1,0}(x) =& h(\bar{L} - h(\bar{L}^2 - 2\bar{L}^*) \\
&+ h^2(3 + \bar{L}^3 - 3|\bar{L}|^2) - h^3(4\bar{L} + \bar{L}^4 - 4\bar{L}^2\bar{L}^* + 2(\bar{L}^*)^2) \\
&+ h^4(5\bar{L}^2 + \bar{L}^5 - 5\bar{L}^* - 5\bar{L}^3\bar{L}^* + 5\bar{L}(\bar{L}^*)^2) \\
&+ h^5(3 + 6\bar{L}^3 + \bar{L}^6 - 12|\bar{L}|^2 - 6\bar{L}^4\bar{L}^* + 9|\bar{L}|^4 - 2(\bar{L}^*)^3)) \\
&+\delta L_x\ (h - 2h^2\bar{L} + 3h^3(\bar{L}^2 - \bar{L}^*) - 4h^4(1 + \bar{L}^3 - 2|\bar{L}|^2) \\
&+ 5h^5(2\bar{L} + \bar{L}^4 - 3\bar{L}^2\bar{L}^* + (\bar{L}^*)^2) \\
&- 6h^6(3\bar{L}^2 + \bar{L}^5 - 2\bar{L}^* - 4\bar{L}^3\bar{L}^* + 3\bar{L}(\bar{L}^*)^2)) \\
&+\delta L_x^*\ (h^2(2 - 3h\bar{L} + 4h^2(\bar{L}^2 - \bar{L}^*) - 5h^3(1 + \bar{L}^3 - 2|\bar{L}|^2) \\
&+ 6h^4(2\bar{L} + \bar{L}^4 - 3\bar{L}^2\bar{L}^* + (\bar{L}^*)^2))) + \mathcal{O}(\delta L^2)
\end{aligned}
\tag{5.6}
$$

$$
\coloneqq\ a_0(h, \bar{L}, \bar{L}^*) + a_1(h, \bar{L}, \bar{L}^*)\delta L_x + a_2(h, \bar{L}, \bar{L}^*)\delta L_x^* + \mathcal{O}(\delta L^2)
$$

Since h, $\bar{L}$ and $\bar{L}^*$ are independent of the sum in the action we are able to rewrite the kinetic fermion action as

$$
\begin{aligned}
\frac{S_{\kappa^2}^{\text{eff}}}{2h_2} &= \sum_x \sum_{i=1}^{3} (a_1\delta L_x + a_2\delta L_x^* + a_0)(a_1\delta L_{x+i} + a_2\delta L_{x+i}^* + a_0) + \mathcal{O}(\delta L^2) \\
&= \sum_x 3(a_0(a_1\delta L_x + a_2\delta L_x^*) + a_0^2) + \sum_{x,i} a_0(a_1\delta L_{x+i} + a_2\delta L_{x+i}^*) + \mathcal{O}(\delta L^2).
\end{aligned}
\tag{5.7}
$$

Due to periodic boundary conditions in all spatial directions we can perform the second sum. We end up with

$$
S_{\kappa^2}^{\text{eff}} = 2h_2 \sum_x \left(6a_0(a_1\delta L_x + a_2\delta L_x^*) + 3a_0^2\right) + \mathcal{O}(\delta L^2). \tag{5.8}
$$

As one can see this action is now a sum over single lattice sites. Hence, the partition function factorizes. After reinserting $\delta L_x = L_x - \bar{L}$ and neglecting terms which do not depend on L_x and L_x^* we obtain the single-site version of the κ^2 action in the heavy dense limit.

$$
S_{\kappa^2}^{\text{eff}} = \sum_x \underbrace{12h_2\ a_0(h, \bar{L}, \bar{L}^*)\left(a_1(h, \bar{L}, \bar{L}^*)\ L_x + a_2(h, \bar{L}, \bar{L}^*)\ L_x^*\right)}_{S_{\kappa^2}^{\text{ss}}} + \mathcal{O}(\delta L^2) \tag{5.9}
$$

This expression can be combined with the static determinant (equation 4.24) and the gauge action (equation 4.11) to obtain the single-site partition function with κ^2 corrections.

$$
\begin{aligned}
Z &= \prod_x Z_{\text{ss}} = (Z_{\text{ss}})^{3N_s} \\
&= \left[\int dL \exp\left\{-(S_{\text{ss}}^g[\lambda, L, L^*] + S_0[h, \overline{h}, L, L^*] + S_{\kappa^2}^{\text{ss}}[h, \overline{h}, h_2, L, L^*])\right\}\right]^{3N_s}
\end{aligned}
\tag{5.10}
$$

As pointed out in [12] to circumvent the issue of dealing with two different mean fields $\bar{L}$ and $\bar{L}^*$ we first compute the expectation value of L in the quenched limit, where we

set $\bar{L} = \langle L \rangle_q = \langle L^* \rangle_q = \bar{L}^*$. Then we obtain a self consistent equation by minimizing the single-site free energy with respect to the mean field.

$$\begin{aligned}
-\frac{\partial F_{\text{ss}}}{\partial \bar{L}} =& \frac{\partial \ln Z_{\text{ss}}}{\partial \bar{L}} \\
=& -\frac{12h_2}{Z_{\text{ss}}} \int dL \left\{ (\frac{\partial(a_0 a_1)}{\partial \bar{L}} L + \frac{\partial(a_0 a_2)}{\partial \bar{L}} L^*) e^{-(S^g_{\text{ss}} + S_0 + S^{\text{ss}}_{\kappa^2})} \right\} \\
&+ \text{terms from gauge action} \\
=& -12h_2 (\frac{\partial(a_0 a_1)}{\partial \bar{L}} \langle L \rangle_{\text{ss}} + \frac{\partial(a_0 a_2)}{\partial \bar{L}} \langle L^* \rangle_{\text{ss}}) + \text{terms from gauge action} \\
\stackrel{!}{=}& -12h_2 (\frac{\partial(a_0 a_1)}{\partial \bar{L}^*} \bar{L} - \frac{\partial(a_0 a_2)}{\partial \bar{L}^*} \bar{L}) + \text{terms from gauge action}
\end{aligned} \tag{5.11}$$

$\bar{L}$ is now obtained by finding a root for this equation. Since F_{mf} has to be minimized the second derivative of F_{mf} has to be positive.

$$\frac{\partial F_{\text{mf}}}{\partial \bar{L}} = 12h_2 (\frac{\partial(a_0 a_1)}{\partial \bar{L}} \langle L \rangle_{\text{ss}} + \frac{\partial(a_0 a_2)}{\partial \bar{L}} \langle L^* \rangle_{\text{ss}} - \frac{\partial(a_0 a_1)}{\partial \bar{L}} \bar{L} - \frac{\partial(a_0 a_2)}{\partial \bar{L}} \bar{L}) = 0 \tag{5.12}$$

The result gives us the expectation value of the Polyakov loop in the quenched phase $\bar{L}_0$. The expectation value in the non-quenched phase is now computed in the following way:

$$\begin{aligned}
\langle L \rangle =& \frac{1}{Z_{\text{ss}}[\bar{L}_0]} \int dL \left\{ L \; e^{-S_{\text{ss}}[\bar{L}_0, L, L^*]} \right\} \\
\langle L^* \rangle =& \frac{1}{Z_{\text{ss}}[\bar{L}_0]} \int dL \left\{ L^* \; e^{-S_{\text{ss}}[\bar{L}_0, L, L^*]} \right\}
\end{aligned} \tag{5.13}$$

The expectation values of the Polyakov loops have to be self-consistent ($\langle L \rangle_{\text{ss}} = \bar{L}$ and $\langle L^* \rangle_{\text{ss}} = \bar{L}^*$). The gauge terms are the same as in equation 4.15. Now the mean field free energy F_{mf} can be constructed from the correct minimum.

$$F_{\text{mf}} = -\ln Z_{\text{ss}} + \overline{F} \tag{5.14}$$

with

$$\frac{\partial F_{\text{mf}}}{\partial \bar{L}} = 12h_2 (\frac{\partial(a_0 a_1)}{\partial \bar{L}} \langle L \rangle_{\text{ss}} + \frac{\partial(a_0 a_2)}{\partial \bar{L}} \langle L^* \rangle_{\text{ss}} - \frac{\partial(a_0 a_1)}{\partial \bar{L}} \bar{L} - \frac{\partial(a_0 a_2)}{\partial \bar{L}} \bar{L}) \stackrel{!}{=} 0. \tag{5.15}$$

In the last expression we did not consider the derivatives of the gauge action terms since they are the same as in equation 4.18. To find non-trivial solutions we can rewrite it as

$$\frac{\partial \overline{F}}{\partial \bar{L}} = -12h_2 (\frac{\partial(a_0 a_1)}{\partial \bar{L}} \bar{L} + \frac{\partial(a_0 a_2)}{\partial \bar{L}} \bar{L}). \tag{5.16}$$

This differential equation for the κ^2 corrections can be evaluated.

$$\begin{aligned}
-\overline{F} = 12h_2(&-\frac{11}{2}h^{12}\bar{L}^{12} + \left(60h^{12} + 10h^{11}\right)\bar{L}^{11} \\
&+ \left(-243h^{12} - 99h^{11} - \frac{27h^{10}}{2}\right)\bar{L}^{10} \\
&+ \left(400h^{12} + 352h^{11} + 120h^{10} + 16h^{9}\right)\bar{L}^{9} \\
&+ \left(-\frac{63h^{12}}{2} - 462h^{11} - \frac{735h^{10}}{2} - 126h^{9} - \frac{35h^{8}}{2}\right)\bar{L}^{8} \\
&+ \left(-648h^{12} - 132h^{11} + 360h^{10} + 324h^{9} + 120h^{8} + 18h^{7}\right)\bar{L}^{7} \\
&+ \left(485h^{12} + 775h^{11} + \frac{515h^{10}}{2} - 205h^{9}\right. \\
&\qquad \left. - 255h^{8} - 100h^{7} - \frac{25h^{6}}{2}\right)\bar{L}^{6} \\
&+ \left(264h^{12} - 328h^{11} - 568h^{10} - 308h^{9}\right. \\
&\qquad \left. + 100h^{8} + 152h^{7} + 56h^{6} + 8h^{5}\right)\bar{L}^{5} \\
&+ \left(-297h^{12} - 285h^{11} + \frac{105h^{10}}{2} + 339h^{9}\right. \\
&\qquad \left. + 207h^{8} - \frac{117h^{6}}{2} - 27h^{5} - \frac{9h^{4}}{2}\right)\bar{L}^{4} \\
&+ \left(-24h^{12} + 150h^{11} + 170h^{10} + 50h^{9} - 124h^{8}\right. \\
&\qquad \left. - 102h^{7} - 16h^{6} + 16h^{5} + 10h^{4} + 2h^{3}\right)\bar{L}^{3} \\
&+ \left(36h^{12} + 15h^{11} - \frac{37h^{10}}{2} - 65h^{9} - 26h^{8} + 16h^{7}\right. \\
&\qquad \left. + 22h^{6} + 7h^{5} - 2h^{4} - 2h^{3} - \frac{h^{2}}{2}\right)\bar{L}^{2})
\end{aligned} \tag{5.17}$$

This is now a power series in the mean field which can be interpreted with Landau's theory of phase transitions. From here, we proceed as in the previous section and compute equation 5.14 and the expectation values for the Polyakov loop (equation 5.13). Results can be found in section 7.

5.2 κ^4 corrections

As shown before we are able to derive mean field expressions in the heavy dense case for higher orders in κ. In this section we will continue with κ^4 corrections. Starting point is the effective action for κ^4 corrections in the heavy dense limit (equation 3.33). We will proceed term by term. The first term is given as

$$S_{\kappa^4,1} = -2h_2^2 \sum_{x,i} W_{1,1}(x) W_{1,1}(x+i). \tag{5.18}$$

The $W_{1,1}$ can be rewritten in terms of Polyakov loops (Appendix A.2) and expanded up to $\mathcal{O}(h^6)$ without any approximations. Then we insert the mean field ansatz and

neglect higher order terms in δL.

$$
\begin{aligned}
W_{1,1}(x) =& \frac{h(L_x + 4h^3 L_x + 4hL_x^* + h^4 L_x + h^2(9 + L_x L_x^*))}{(1 + hL_x + h^2 L_x^* + h^3)^2} \\
=& hL_x + h^2(4L_x^* - 2L_x^2) + 3h^3(3 + L_x^3 - 3|L_x|^2) \\
& - 4h^4(4L_x + L_x^4 - 4L_x^2 L_x^* + 2(L_x^*)^2) \\
& + h^5(L_x + 25L_x^2 + 5L_x^5 - 26L_x^* - 25L_x^3 L_x^* + 25L_x(L_x^*)^2) \\
& - 2h^6(9 + L_x^2 + 18L_x^3 + 3L_x^6 - 37|L_x|^2 - 18L_x^4 L_x^* \\
& \qquad + 27|L_x|^4 - 6(L_x^*)^3) \\
=& \quad h\bar{L} - 2h^2(\bar{L}^2 - 2\bar{L}^*) + 3h^3(3 + \bar{L}^3 - 3|\bar{L}|^2) \\
& \quad - 4h^4(4\bar{L} + \bar{L}^4 - 4\bar{L}^2\bar{L}^* + 2(\bar{L}^*)^2) \\
& \quad + h^5(\bar{L} + 25\bar{L}^2 + 5\bar{L}^5 - 26\bar{L}^* - 25\bar{L}^3\bar{L}^* + 25\bar{L}(\bar{L}^*)^2) \\
& \quad - 2h^6(9 + \bar{L}^2 + 18\bar{L}^3 + 3\bar{L}^6 - 37|\bar{L}|^2 - 18\bar{L}^4\bar{L}^* \\
& \quad + 27|\bar{L}|^4 - 6(\bar{L}^*)^3) \\
& + \delta L_x^* \, (4h^2 - 26h^5 - 9h^3\bar{L} + 74h^6\bar{L}^2 - 25h^5\bar{L}^3 + 36h^6\bar{L}^4 \\
& \qquad - 16h^4\bar{L}^* + 50h^5|\bar{L}|^2 - 108h^6\bar{L}^2\bar{L}^* + 36h^6(\bar{L}^*)^2) \\
& + \delta L_x \, (h - 16h^4 + h^5 - 4h^2\bar{L} - 4h^6\bar{L} + 9h^3\bar{L}^2 - 108h^6\bar{L}^2 \\
& \qquad - 16h^4\bar{L}^3 + 25h^5\bar{L}^4 - 36h^6\bar{L}^5 - 9h^3\bar{L}^* + 74h^6\bar{L}^* \\
& \qquad + 32h^4|\bar{L}|^2 - 75h^5\bar{L}^2\bar{L}^* + 144h^6\bar{L}^3\bar{L}^* \\
& \qquad + 25h^5(\bar{L}^*)^2 - 108h^6\bar{L}(\bar{L}^*)^2) + \mathcal{O}(\delta L^2) \\
\coloneqq& \, b_0 + b_1\delta L_x + b_2\delta L_x^* + \mathcal{O}(\delta L^2)
\end{aligned}
\tag{5.19}
$$

If we insert the last expression in equation 5.18, even more terms can be neglected.

$$
\begin{aligned}
-\frac{S_{\kappa^4,1}}{2h_2^2} &= \sum_{x,i} \left((b_0 + b_1\delta L_x + b_2\delta L_x^*)(b_0 + b_1\delta L_{x+i} + b_2\delta L_{x+i}^*) \right) + \mathcal{O}(\delta L^2) \\
&= \sum_{x,i} (b_0^2 + b_0(b_1\delta L_x + b_2\delta L_x^* + b_1\delta L_{x+i} + b_2\delta L_{x+i}^*)) + \mathcal{O}(\delta L^2)
\end{aligned}
\tag{5.20}
$$

We split up the sum into terms which only contain a sum over the lattice site and terms containing neighboring sites. Then we perform the sum over the neighboring sites and relabel the indices.

$$
\begin{aligned}
& \sum_x 3(b_0^2 + b_0(b_1\delta L_x + b_2\delta L_x^*)) + \sum_x \sum_{i=1}^{3} (b_0(b_1\delta L_{x+i} + b_2\delta L_{x+i}^*)) \\
=& \sum_x 3(b_0^2 + 2b_0(b_1\delta L_x + b_2\delta L_x^*))
\end{aligned}
\tag{5.21}
$$

After the reinsertion of the Polyakov loops the expression for the first term of the κ^4 corrections up to constant terms, which factor out in the partition sum, has the form

$$-S_{\kappa^4,1} = \sum_x \underbrace{12h_2^2(b_0b_1L_x + b_0b_2L_x^*)}_{-S^{\mathrm{ss}}_{\kappa^4,1}} + \mathrm{const} + \mathcal{O}(\delta L^2). \tag{5.22}$$

We continue with the second term from equation 3.33

$$-S_{\kappa^4,2} = h_2^2 \sum_{x,i,j} W_{1,1}(x)W_{1,0}(x-i)W_{1,0}(x-j). \tag{5.23}$$

Inserting equation 5.6 and 5.19 we find

$$\begin{aligned}
-\frac{S_{\kappa^4,2}}{h_2^2} =& \sum_{x,i,j}(b_0 + b_1\delta L_x + b_2\delta L_x^*)(a_0 + a_1\delta L_{x-i} + a_2\delta L_{x-i}^*) \\
&\qquad \times (a_0 + a_1\delta L_{x-j} + a_2\delta L_{x-j}^*) + \mathcal{O}(\delta L^2) \\
=& \sum_{x,i,j} \big(a_0^2b_0 + a_0^2(b_1\delta L_x + b_2\delta L_x^*) \\
&+ a_0b_0(a_1\delta L_{x-i} + a_2\delta L_{x-i}^* + a_1\delta L_{x-j} + a_2\delta L_{x-j}^*)\big) + \mathcal{O}(\delta L^2) \\
=& \sum_x 9(a_0^2b_0 + a_0^2(b_1\delta L_x + b_2\delta L_x^*)) \\
&+ 3\sum_x (a_0b_0(a_1(\underbrace{\delta L_{x-1} + \delta L_{x-2} + \delta L_{x-3}}_{=3\ \delta L_x}) \\
&\quad + 2a_2(\underbrace{\delta L_{x-1}^* + \delta L_{x-2}^* + \delta L_{x-3}^*}_{=3\ \delta L_x^*}))) \\
&\quad + \mathcal{O}(\delta L^2) \\
=& 9\sum_x \big((a_0^2b_0 + a_0^2(b_1\delta L_x + b_2\delta L_x^*)) + 2(a_0b_0(a_1\delta L_x + a_2\delta L_x^*))\big) \\
&+ \mathcal{O}(\delta L^2) \\
=& 9\sum_x \big[a_0^2b_0 + (a_0^2b_1 + 2a_0b_0a_1)\delta L_x + (a_0^2b_2 + 2a_0b_0a_2)\delta L_x^*\big] + \mathcal{O}(\delta L^2).
\end{aligned} \tag{5.24}$$

L_x is reinserted and independent terms are dropped. Then, the action reads

$$-S_{\kappa^4,2} = \sum_x \underbrace{9h_2^2[(a_0^2b_1 + 2a_0b_0a_1)L_x + (a_0^2b_2 + 2a_0b_0a_2)L_x^*]}_{-S^{\mathrm{ss}}_{\kappa^4,2}} + \mathcal{O}(\delta L^2). \tag{5.25}$$

The third term of the κ^4 corrections is given as

$$-S_{\kappa^4,3} = 2h_2^2 \sum_{x,i,j} W_{1,1}(x)W_{1,0}(x-i)W_{1,0}(x+j). \tag{5.26}$$

Although the signs in the indices of the neighboring sites are different it gives the same contribution with an extra factor of two as the second term (equation 5.24).

$$\begin{aligned}
-\frac{S_{\kappa^4,3}}{2h_2^2} =& \sum_{x,i,j}(b_0 + b_1\delta L_x + b_2\delta L_x^*)(a_0 + a_1\delta L_{x-i} + a_2\delta L_{x-i}^*) \\
&\qquad \times (a_0 + a_1\delta L_{x+j} + a_2\delta L_{x+j}^*) + \mathcal{O}(\delta L^2) \\
=& \sum_{x,i,j} \big(a_0^2 b_0 + a_0^2(b_1\delta L_x + b_2\delta L_x^*) \\
&+ a_0 b_0(a_1\delta L_{x-i} + a_2\delta L_{x-i}^* + a_1\delta L_{x-j} + a_2\delta L_{x-j}^*)\big) + \mathcal{O}(\delta L^2) \\
=& \sum_x 9(a_0^2 b_0 + a_0^2(b_1\delta L_x + b_2\delta L_x^*)) \\
&+ 3\sum_x (a_0 b_0(a_1(\underbrace{\delta L_{x-1} + \delta L_{x-2} + \delta L_{x-3} + \delta L_{x+1} + \delta L_{x+2} + \delta L_{x+3}}_{=6\ \delta L_x}) \\
&\quad + a_2(\underbrace{\delta L_{x-1}^* + \delta L_{x-2}^* + \delta L_{x-3}^* + \delta L_{x+1}^* + \delta L_{x+2}^* + \delta L_{x+3}^*}_{=6\ \delta L_x^*}))) \\
&\quad + \mathcal{O}(\delta L^2) \\
=& 9\sum_x \left[a_0^2 b_0 + (a_0^2 b_1 + 2a_0 b_0 a_1)\delta L_x + (a_0^2 b_2 + 2a_0 b_0 a_2)\delta L_x^*\right] + \mathcal{O}(\delta L^2)
\end{aligned} \tag{5.27}$$

Thus, the single-site action for the third term is

$$-S_{\kappa^4,3} = \sum_x \underbrace{18h_2^2[(a_0^2 b_1 + 2a_0 b_0 a_1)L_x + (a_0^2 b_2 + 2a_0 b_0 a_2)L_x^*]}_{-S_{\kappa^4,3}^{\text{ss}}} + \mathcal{O}(\delta L^2). \tag{5.28}$$

The same applies to the fourth term which is the same as equation 5.24 with flipped indices.

$$\begin{aligned}
-S_{\kappa^4,4} =& h_2^2 \sum_{x,i,j} W_{1,1}(x)W_{1,0}(x+i)W_{1,0}(x+j) \\
=& \sum_x \underbrace{9h_2^2[(a_0^2 b_1 + 2a_0 b_0 a_1)L_x + (a_0^2 b_2 + 2a_0 b_0 a_2)L_x^*]}_{-S_{\kappa^4,4}^{\text{ss}}} + \mathcal{O}(\delta L^2)
\end{aligned} \tag{5.29}$$

Adding equation 5.22, 5.24, 5.27, and 5.29 up returns the single-site mean field action for the κ^4 corrections. We drop the lattice site index.

$$\begin{aligned}
-S_{\kappa^4}^{\text{ss}} =& -(S_{\kappa^4,1}^{\text{ss}} + S_{\kappa^4,2}^{\text{ss}} + S_{\kappa^4,3}^{\text{ss}} + S_{\kappa^4,4}^{\text{ss}}) \\
=& 12h_2^2(b_0 b_1 L + b_0 b_2 L^*) + 36h_2^2[(a_0^2 b_1 + 2a_0 b_0 a_1)L + (a_0^2 b_2 + 2a_0 b_0 a_2)L^*] \\
=& 12h_2^2\left((b_0 b_1 + 3(a_0^2 b_1 + 2a_0 b_0 a_1))L + (b_0 b_2 + 3(a_0^2 b_2 + 2a_0 b_0 a_2))L^*\right)
\end{aligned} \tag{5.30}$$

As done before, we check for self-consistency by taking the derivative of the single-site free energy in the quenched approximation ($\bar{L} = \bar{L}^*$).

$$\begin{aligned}
\frac{\partial F_{\mathrm{ss}}^{\kappa^4}}{\partial \bar{L}} =& -\frac{\partial \ln Z_{\mathrm{ss}}^{\kappa^4}(\bar{L})}{\partial \bar{L}} = -\frac{12h_2^2}{Z_{\mathrm{ss}}(\bar{L})}\int dL \Bigg[\Bigg(b_0\frac{\partial b_1}{\partial \bar{L}} + b_1\frac{\partial b_0}{\partial \bar{L}} + 3(2a_0b_1\frac{\partial a_0}{\partial \bar{L}} \\
&+a_0^2\frac{\partial b_1}{\partial \bar{L}} + 2(b_0a_1\frac{\partial a_0}{\partial \bar{L}} + a_1a_0\frac{\partial b_0}{\partial \bar{L}} + a_0b_0\frac{\partial a_1}{\partial \bar{L}}))\Bigg) L \\
&+\Bigg(b_0\frac{\partial b_2}{\partial \bar{L}} + b_2\frac{\partial b_0}{\partial \bar{L}} + 3(2a_0b_2\frac{\partial a_0}{\partial \bar{L}} + a_0^2\frac{\partial b_2}{\partial \bar{L}} \\
&+2(b_0a_2\frac{\partial a_0}{\partial \bar{L}} + a_2a_0\frac{\partial b_0}{\partial \bar{L}} + a_0b_0\frac{\partial a_2}{\partial \bar{L}}))\Bigg))L^*\Bigg] \exp[-S_{\kappa^4}^{\mathrm{ss}}(\bar{L})] \\
\stackrel{!}{=} -12h_2^2&\Bigg[\Bigg(b_0\frac{\partial b_1}{\partial \bar{L}} + b_1\frac{\partial b_0}{\partial \bar{L}} + 3(2a_0b_1\frac{\partial a_0}{\partial \bar{L}} + a_0^2\frac{\partial b_1}{\partial \bar{L}} \\
&+2(b_0a_1\frac{\partial a_0}{\partial \bar{L}} + a_1a_0\frac{\partial b_0}{\partial \bar{L}} + a_0b_0\frac{\partial a_1}{\partial \bar{L}}))\Bigg) \bar{L} \\
&+\Bigg(b_0\frac{\partial b_2}{\partial \bar{L}} + b_2\frac{\partial b_0}{\partial \bar{L}} + 3(2a_0b_2\frac{\partial a_0}{\partial \bar{L}} + a_0^2\frac{\partial b_2}{\partial \bar{L}} \\
&+2(b_0a_2\frac{\partial a_0}{\partial \bar{L}} + a_2a_0\frac{\partial b_0}{\partial \bar{L}} + a_0b_0\frac{\partial a_2}{\partial \bar{L}}))\Bigg))\bar{L}\Bigg] = -\frac{\partial \bar{F}^{\kappa^4}}{\partial \bar{L}}
\end{aligned} \tag{5.31}$$

The solution to this equation is the mean field $\bar{L}_0$ in the quenched phase which minimizes the mean field free energy $F_{\mathrm{mf}}^{\kappa^4}$. It is defined as

$$F_{\mathrm{mf}}^{\kappa^4} = \ln Z_{\mathrm{ss}}^{\kappa^4} + \bar{F}^{\kappa^4}. \tag{5.32}$$

The symbolic expression for $\bar{F}^{\kappa^4}$ can be looked up in the appendix. From here, expectation values in the non-quenched case can be calculated.
The non-quenched Polyakov Loop expectation values are given as

$$\begin{aligned}
\langle L \rangle =& \frac{1}{Z_{\mathrm{ss}}[\bar{L}_0]}\int dL \left\{L\ e^{-S_{\mathrm{ss}}[\bar{L}_0, L, L^*]}\right\} \\
\langle L^* \rangle =& \frac{1}{Z_{\mathrm{ss}}[\bar{L}_0]}\int dL \left\{L^*\ e^{-S_{\mathrm{ss}}[\bar{L}_0, L, L^*]}\right\}.
\end{aligned} \tag{5.33}$$

$S_{\mathrm{ss}}[\bar{L}_0, L, L^*]$ contains the κ^2 and κ^4 single-site action.

6 Roberge-Weiss transition

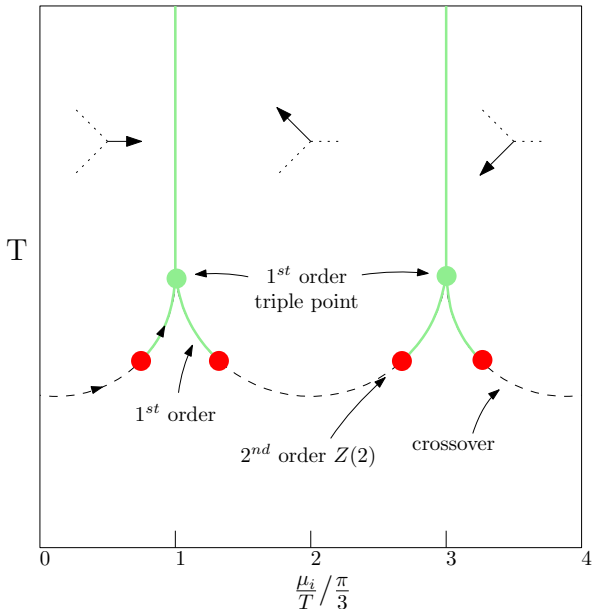

Figure 11: Schematic QCD phase diagram at imaginary chemical potential for intermediate quark masses from [13].

Due to the sign problem, it is impossible to evaluate full lattice QCD at finite chemical potential μ. Nevertheless, it is solvable for a purely imaginary chemical potential $\mu = i\mu_I$. In this region QCD exhibits another symmetry which is called Roberge-Weiss symmetry. It is related to the center symmetry which is fulfilled in pure gauge theory. As we saw in section 4.2 fermions break the center symmetry explicitly. However, the symmetry can be maintained for certain quark masses when considering an imaginary chemical potential. In this section we want to study if the Roberge-Weiss transition was realized in the mean field study and compare our results to previous works [11]. The phase diagram for imaginary chemical potential is divided into three different sectors. These sectors correspond to the center sectors of the Polyakov loop. This is shown in figure 11. They are separated by first order phase transitions. For smaller quark masses the transition turns at low temperature into a crossover (dotted line). The first order transition between neighboring sectors ends in a critical point, where the phase transition becomes second order. These critical points get shifted to higher temperatures into the direction of the bifurcation point when the quark mass is decreased. At a certain mass the bifurcation point and two critical points meet. There, the first order transition ends in a tricritical point.
Now, we want to study the effective theory in the mean field approach at imaginary

potential. We can write equation 3.30 in the following way:

$$\begin{aligned} h &= (2\kappa)^{N_\tau}(\cos(N_\tau a\mu_I) + i\sin(N_\tau a\mu_I)) \\ \overline{h} &= (2\kappa)^{N_\tau}(\cos(N_\tau a\mu_I) - i\sin(N_\tau a\mu_I)) \end{aligned} \tag{6.1}$$

$$\Leftrightarrow h = \overline{h}^*$$

It is convenient to make a change of variables. We substitute $\theta = N_\tau a\mu_I = \mu_I/T$ and $h_0 = (2\kappa)^{N_\tau}$. One can see that this makes the partition function periodic in θ. Next, we proceed analogously to section 4.2. We compute the single-site partition function and the mean field free energy (equation 4.26). We fix λ and h_0 to the phase transition points discovered in section 4.2. Since we checked that higher orders in κ are negligible we proceed only with the static determinant from equation 4.24. We vary θ and examine how the transition behaves. The critical endpoint of the first order line increases to higher values of h_0. This turns out to be valid until we reach the critical value of $\theta = \pi/3$. There, one reaches the tricritical point which is the endpoint of the boundary between two neighboring Polyakov loop sectors. They are separated by a first order transition. The shift in the critical point is shown in figure 12 and was determined by searching for the point where the first and second derivative of the mean field free energy F_{mf} is zero. Since we plot F_{mf} in terms of the real part of $\overline{L}$ the method is only sensitive to the first Polyakov sector which is located on the real axis. This is realized for $-\pi/3 \leq \theta \leq \pi/3$. The critical effective gauge coupling λ_{crit} is not effected by the chemical potential. $\lambda_{\text{cp}}(\theta) \approx 0.1594$.
To compare our results we use the approximation for the quark mass M from [9] to compute M/T. For heavy quarks and one flavor the following relation is valid:

$$\frac{M}{T} = -\ln(h_0) \tag{6.2}$$

In [11] it is shown that we can fit the mass with the following function to our data based on an expansion for real chemical potential:

$$\frac{M}{T} = -\ln\left(\frac{D}{\cosh(\mu/T)}\right) \tag{6.3}$$

For our results we obtain $D = 0.00065(3)$ with a reduced $\chi^2 = 2.4 \times 10^{-6}$. This is a relative deviation of the numerical computations of 13%.
Besides the fit from analytic continuation of real chemical potential we compare our results to tricritical scaling. Therefore we use the two-parameter fit from [14].

$$\frac{M}{T} = \frac{M_{\text{tric}}}{T} + K\left[\left(\frac{\pi}{3}\right)^2 + \left(\frac{\mu}{T}\right)^2\right]^{2/5} \tag{6.4}$$

We obtain $\frac{M_{\text{tric}}}{T} = 6.56 \pm 0.04$ and $K = 0.69 \pm 0.05$. The deviation compared to the results in [11] is 20%. The results plotted on $(\frac{\mu}{T})^2$ are shown in figure 13. One can immediately see that the mean field approach does not show tricritical scaling. This agrees with other results from mean field theory which fails when computing universal

behavior [1].
The analytic continuation matches the results from the mean field approach. This is in contridiction with the results in [11] which show a very good agreement with the tricritical scaling. The reason is that for universal behavior fluctuations, which were neglected in mean field theory, become important. Thus, we do not observe tricritical scaling but nearly a linear relation between M/T and $(\mu/T)^2$.

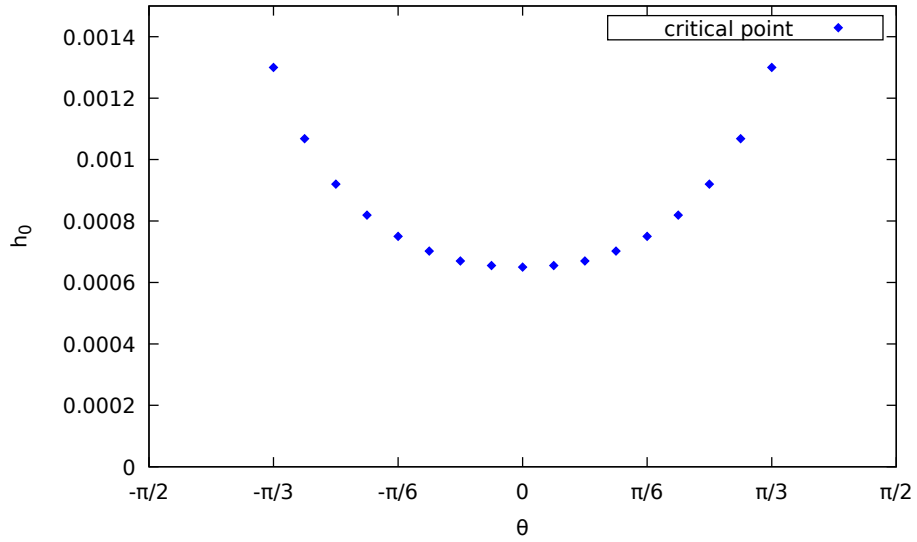

Figure 12: The change of the critical endpoint with imaginary chemical potential $\theta = \mu_I/T$.

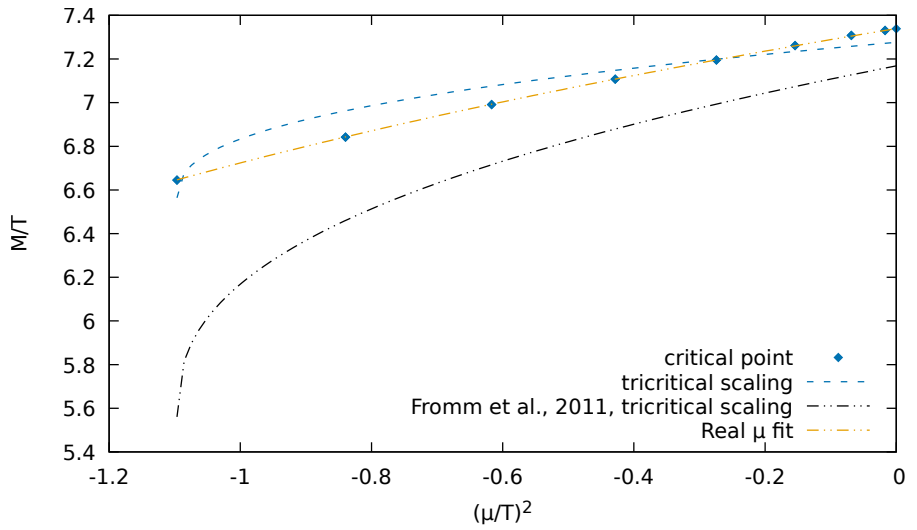

Figure 13: Scaling of $\frac{M}{T}$ for one flavor. The curves are the fittings from real-μ and tricritical scaling.

7 Liquid-gas transition to nuclear matter

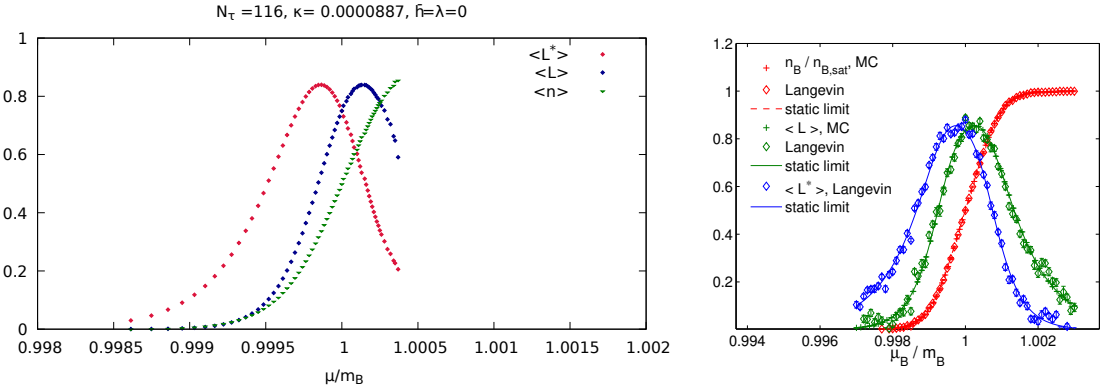

Figure 14: Expectation values for the Polyakov loop up to κ^2 corrections and the baryon density ($N_\tau = 116$, $\kappa = 0.0000887$). The mean field results (left) and the results from Monte Carlo and Langevin calculations [15](right).

At low temperatures nuclear matter forms a hadron gas. This state changes when the chemical potential is increased. When the chemical potential reaches approximately the baryon rest mass, the quarks form nuclei, which can be interpreted as droplets. This is known as the liquid-gas transition of nuclear matter. In this section we want to study if the developed mean field approach shows this behavior and compare it to previous works [15, 7].
Since the liquid-gas transition of nuclear matter occurs in a different parameter region than the deconfinement transition, it is important to estimate the region where the phase transition occurs. In leading order the baryon mass can be written as:

$$am_B \approx -3\ln(2\kappa). \tag{7.1}$$

Now, we can insert this into equation 3.30 and find the following expression:

$$h = e^{\frac{\mu - m_B/3}{T}}. \tag{7.2}$$

Since the transition occurs when the chemical potential reaches the baryon mass ($\mu_B = 3\mu \approx m_B$), h has to be around 1. Aside from that, $\bar{h} \to 0$. Thus, anti-quarks are suppressed in this region. The temperature T should be small, which means that N_τ is large. Since h is not small in the heavy dense quark region, also kinetic terms of the quark determinant contribute. Thus we consider κ^2 and κ^4 corrections in this section. μ can be calculated in the following way.

$$\begin{aligned} a\mu &= -\frac{\ln h}{3N_\tau} - \ln(2\kappa) \\ \Leftrightarrow \frac{\mu_B}{m_B} &= 1 - \frac{\ln(h)}{N_\tau \ln(2\kappa)} \end{aligned} \tag{7.3}$$

The density is computed via the relation from statistical physics. It is given as the derivative of the grand canonical potential with respect to the chemical potential.

$$\begin{aligned} n &= -T\frac{\partial \ln Z_{\text{ss}}}{\partial \mu} \\ &= -T\frac{\partial \ln Z_{\text{ss}}}{\partial h}\frac{\partial h}{\partial \mu} \\ &= -h\frac{\partial \ln Z_{\text{ss}}}{\partial h} \end{aligned} \tag{7.4}$$

$$n = 3n_B \tag{7.5}$$

The expectation values for L and L^* are calculated with equation 5.13 and 5.33 for the respective cases. The results for the liquid-gas transition of the effective theory including κ^2 corrections are shown in figure 14. As one can see, the Polyakov loop expectation value as well as the baryon number density indicate a crossover from the hardronic to the nuclei phase. This is coherent with the results in [15]. At low chemical potential the baryon density n_B is zero. It changes to a finite value around the baryon mass m_B. At this point nuclei form. Since we observe a crossover the temperature has to be too high to see the true phase transition shown in figure 3a. Since we are in the limit of very heavy quarks (small κ) the critical transition is shifted approximately to zero temperature.
The number density including κ^4 corrections for different temperatures are shown in figure 15. The results for the mean field analysis are mainly reliant on the convergence of the self-consistency condition (equation 5.15). This gets more computationally expensive for larger chemical potentials since the expectation values have to be expanded to higher orders for larger chemical potential μ. Nevertheless, mean field theory is able to reproduce the liquid-gas transition qualitatively.

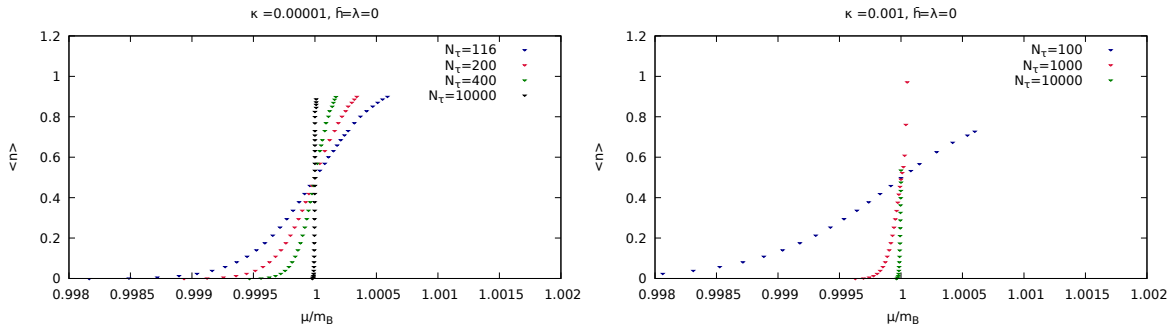

Figure 15: The liquid-gas transition of nuclear matter for different temperatures and two different hopping parameters.

8 Conclusion

In this thesis we developed a mean field approach to different Polyakov loop theories. Those were directly derived from lattice QCD. This study allowed for an analytic access to the models. The mean field analysis has the advantage of not suffering from the sign problem. It therefore allows us to study the finite μ region. We produced results which were in good agreement with lattice results not only in a qualitative but also in a quantitative way. We studied the deconfinement phase transition with Landau's theory of phase transitions. The transition is of first order with the Polyakov loop as true order parameter for pure gauge theory. The associated symmetry is center symmetry. We introduced fermions in the heavy quark mass limit and studied their influence on the deconfinement transition. The first order transition weakened and ended in a critical point where the transition became second order due to the explicit breaking of center symmetry of fermions.
The region of imaginary chemical potential was studied. We were able to link the deconfinement transition to the Roberge-Weiss transition although the mean field study did not show tricritical scaling which is the universality class of these Polyakov models. Therefore fluctuations have to be considered.
Furthermore, we demonstrated how to include kinetic quark contributions into the mean field analysis. The expressions for κ^2 and κ^4 corrections in the heavy dense limit were derived. This method can be extended to higher order terms. We explored the finite density region in the heavy dense limit and observed the liquid-gas transition of nuclear matter. The transition was observed as a crossover.
We showed that mean field theory can be applied to these Polyakov theories. It gives qualitative results and gives analytic access to the effective theory. The approach shows great promise for a simple access to the theory. As a result, the influence of other correction terms can be estimated without great effort.

A Appendix

A.1 Polyakov loop integrals

To evaluate the single-site partition function introduced in equation 4.11 one has to compute integrals of the following kind:

$$\int dL\ e^{aL+bL^*} \tag{A.1}$$

Unfortunately, there is no analytical solution to this integral. Nevertheless, the exponential series converges. Hence, we rewrite the exponential in its series expansion form:

$$e^{aL+bL^*} = \sum_{k=0}^{\infty} \frac{(aL+bL^*)^k}{k!} \tag{A.2}$$

This series converges due to the factorial factor in the denominator. After expanding the numerator, integrals of the following type have to be evaluated.

$$\int dL\ L^n (L^*)^m \tag{A.3}$$

These integrals can be solved. The technique used in this work was introduced in [16]. For SU(3) only integrals with $(n-m) \mod 3 = 0$ contribute. This can be seen in the multiplet representation of SU(3). All multiplets containing a singlet contribute [17]. As an example the lowest contributing integral is given by

$$\begin{aligned} \int dL\ LL^* &= \int dL \mathrm{tr}(T)\mathrm{tr}(T^\dagger) \\ &= \sum_{a=1,b=1}^{3} \int dL\ T_{aa}T^\dagger_{bb} \\ &= \frac{1}{3}\sum_{a,b} \delta_{ab}\delta_{ab} = 1. \end{aligned} \tag{A.4}$$

For the evaluation of the single-site partition function (equation 4.11) we expand the exponential and computed the Polyakov loop integrals up to convergence. The method was implemented in mathematica.

In the following we state the solutions to the lowest orders of those integrals:

$$\int dL\ LL^* = 1$$
$$\int dL\ L^3 = 1$$
$$\int dL\ L^6 = 5$$
$$\int dL\ L^9 = 42$$
$$\int dL\ (L^*)^3 = 1$$
$$\int dL\ (L^*)^6 = 5$$
$$\int dL\ (L^*)^9 = 42$$
$$\int dL\ L^4L^* = 3$$
$$\int dL\ L^7L^* = 21$$
$$\int dL\ L^2(L^*)^2 = 2$$
$$\int dL\ L^5(L^*)^2 = 11$$
$$\int dL\ L^8(L^*)^2 = 98$$
$$\int dL\ L^3(L^*)^3 = 6$$
$$\int dL\ L^6(L^*)^3 = 47$$
$$\int dL\ L(L^*)^4 = 3$$
$$\int dL\ L^4(L^*)^4 = 23$$
$$\int dL\ L^2(L^*)^5 = 11$$
$$\int dL\ L^5(L^*)^5 = 103$$
$$\int dL\ L^3(L^*)^6 = 47$$
$$\int dL\ L(L^*)^7 = 21$$
$$\int dL\ L^2(L^*)^8 = 98$$

A.2 Reformulation of traces over Wilson lines into Polyakov loops

Each $W_{n,m}$ is a rational of temporal Wilson loops. They can be reformulated in terms of Polyakov loops. Therefore one can compute derivatives of the generating functional $G[\alpha, \beta]$.

$$W_{n,m} = \mathrm{tr}\frac{(h\ W)^n}{(1+h\ W)^{n+m}} = \frac{(-1)^{m+n-1}}{(m+n-1)!}\left(\frac{\partial}{\partial\alpha}\right)^m\left(\frac{\partial}{\partial\beta}\right)^n G[\alpha,\beta]\Big|_{\alpha=\beta=1} \tag{A.5}$$

The generating functional can be constructed from the static determinant via the trace-logarithm relation. It has the following form:

$$G[\alpha,\beta] = \ln\det[\alpha+\beta hW] = \ln[\alpha^3+\alpha^2\beta hL+\alpha\beta^2h^2L^\dagger+\beta^3h^3] \tag{A.6}$$

Now we can compute $W_{1,0}$ and $W_{1,1}$ in terms of Polyakov loops and the effective quark- and anti-quark couplings $(h/\overline{h})$.

$$W_{1,0}(x) = \frac{hL_x+2h^2L_x^*+3h^3}{1+hL_x+h^2L_x^*+h^3} \tag{A.7}$$

$$W_{1,1}(x) = \frac{h(L_x+4h^3L_x+4hL_x^*+h^4L_x^*+h^2(9+L_xL_x^*))}{(1+hL_x+h^2L_x^*+h^3)^2} \tag{A.8}$$

These expressions can be given without any approximation as series in h up to order $h^{2N_fN_c}$.

A.3 Mean field free energy for κ^4 corrections

In the following we wright down the power series in the mean field for κ^4 corrections.

$$-\frac{\bar{F}^{\kappa^4}}{12h_2^2} = \sum_n a_n(h)\ \bar{L}^n$$

All non-zero coefficients are

$$\begin{aligned}
a_2(h) =& 5832h^{18} + 2295h^{17} - 4464h^{16} - 16335h^{15} - 6174h^{14} + 6669h^{13} + 11664h^{12} \\
&+ 4005h^{11} - \frac{4487h^{10}}{2} - 1949h^9 - 475h^8 + 80h^7 + 46h^6 + 11h^5 \\
&+ 8h^4 + 4h^3 + \frac{h^2}{2} \\
a_3(h) =& -3888h^{18} + 41310h^{17} + 45504h^{16} + 8940h^{15} - 69888h^{14} - 64272h^{13} \\
&- 7440h^{12} + 27180h^{11} + 18190h^{10} + 1274h^9 - 2300h^8 - 1122h^7 - 160h^6 \\
&+ 32h^5 + 14h^4 + 2h^3 \\
a_4(h) =& -83106h^{18} - 80325h^{17} + 59616h^{16} + 231525h^{15} + 155736h^{14} - 51246h^{13} \\
&- 130032h^{12} - 60453h^{11} + \frac{16125h^{10}}{2} + 17817h^9 + 6249h^8 + 168h^7 \\
&- \frac{1071h^6}{2} - 177h^5 - 21h^4 \\
a_5(h) =& 73872h^{18} - 249084h^{17} - 408576h^{16} - 207000h^{15} + 291648h^{14} + 378612h^{13} \\
&+ 114912h^{12} - 67908h^{11} - 68008h^{10} - 17180h^9 + 2108h^8 \\
&+ 2712h^7 + 752h^6 + 80h^5 \\
a_6(h) =& 315090h^{18} + 543150h^{17} + 19200h^{16} - 695550h^{15} - 691110h^{14} - 91260h^{13} \\
&+ 243960h^{12} + 170295h^{11} + \frac{61865h^{10}}{2} - 15675h^9 - 9640h^8 - 2200h^7 - \frac{425h^6}{2} \\
a_7(h) =& -396576h^{18} + 339048h^{17} + 1102464h^{16} + 901530h^{15} - 137088h^{14} - 601146h^{13} \\
&- 323568h^{12} - 27522h^{11} + 48480h^{10} + 25596h^9 + 5520h^8 + 462h^7 \\
a_8(h) =& -427518h^{18} - 1312332h^{17} - 748272h^{16} + 499905h^{15} + 991368h^{14} + 485394h^{13} \\
&- 21546h^{12} - 112497h^{11} - \frac{103075h^{10}}{2} - 10836h^9 - 931h^8 \\
a_9(h) =& 866880h^{18} + 376584h^{17} - 930048h^{16} - 1267320h^{15} - 501312h^{14} + 144456h^{13} \\
&+ 213504h^{12} + 87912h^{11} + 17720h^{10} + 1496h^9
\end{aligned}$$

$$
\begin{aligned}
a_{10}(h) =& -26244h^{18} + 1130517h^{17} + 1277424h^{16} + 415125h^{15} - 304668h^{14} \\
& - 342927h^{13} - 131544h^{12} - 25542h^{11} - \frac{4203h^{10}}{2} \\
a_{11}(h) =& -751680h^{18} - 1019490h^{17} - 194880h^{16} + 423000h^{15} + 415800h^{14} \\
& + 173940h^{13} + 33120h^{12} + 2670h^{11} \\
a_{12}(h) =& 485892h^{18} + 561h^{17} - 494736h^{16} - 428505h^{15} - 178332h^{14} \\
& - 38610h^{13} - 3102h^{12} \\
a_{13}(h) =& 81648h^{18} + 436968h^{17} + 387072h^{16} + 162000h^{15} + 35280h^{14} + 3276h^{13} \\
a_{14}(h) =& -242190h^{18} - 281775h^{17} - 129792h^{16} - 29250h^{15} - 2730h^{14} \\
a_{15}(h) =& 133056h^{18} + 84966h^{17} + 21504h^{16} + 2100h^{15} \\
a_{16}(h) =& -36450h^{18} - 13005h^{17} - 1440h^{16} \\
a_{17}(h) =& 5184h^{18} + 816h^{17} \\
a_{18}(h) =& -306h^{18}
\end{aligned}
$$

References

[1] Nigel Goldenfeld. *Lectures on phase trasitions and the renormalization group*. Frountiers in physics. Boulder: Westview Press, 2010.

[2] Michael E. Peskin and Daniel V. Schroeder. *An Introduction To Quantum Field Theory*. Westview Press, 1995.

[3] Christof Gattringer and Christian B. Lang. *Quantum Chromodynamics on the Lattice*. Springer, 2010.

[4] Mathias Neuman. "Effective Theory for Heavy Quark QCD at Finite Temperature and Density with Stochastic Quantization". PhD thesis. Johann Wolfgang Goethe Universität Frankfurt, 2015.

[5] Jonas Glesaaen. "Heavy quark QCD at finite temperature and density using an effective theory". PhD thesis. Johann Wolfgang Goethe Universität Frankfurt, 2016.

[6] Jens Langelage, Stefano Lottini, and Owe Philipsen. "Centre symmetric 3d effective actions for thermal SU(N) Yang-Mills from strong coupling series". In: *Journal of High Energy Physics* 2011, 57 (Feb. 2011), p. 57. DOI: 10.1007/JHEP02(2011)057. arXiv: 1010.0951 [hep-lat].

[7] Jens Langelage, Mathias Neuman, and Owe Philipsen. "Heavy dense QCD and nuclear matter from an effective lattice theory". In: *Journal of High Energy Physics* 2014, 131 (Sept. 2014), p. 131. DOI: 10.1007/JHEP09(2014)131. arXiv: 1403.4162 [hep-lat].

[8] Philippe de Forcrand and Massimo D'Elia. "Continuum limit and universality of the Columbia plot". In: *PoS* LATTICE2016 (2017), p. 081. DOI: 10.22323/1.256.0081. arXiv: 1702.00330 [hep-lat].

[9] John B. Kogut, Michael Snow, and Michael Stone. "Mean field and Monte Carlo studies of SU(N) chiral models in three dimensions". In: *Nuclear Physics B* 200.1 (1982), pp. 211–231. ISSN: 0550-3213. DOI: https://doi.org/10.1016/0550-3213(82)90065-7. URL: http://www.sciencedirect.com/science/article/pii/0550321382900657.

[10] F. Green and F. Karsch. "Mean field analysis of SU(N) deconfining transitions in the presence of dynamical quarks". In: *Nuclear Physics B* 238.2 (1984), pp. 297–306. ISSN: 0550-3213. DOI: https://doi.org/10.1016/0550-3213(84)90452-8. URL: http://www.sciencedirect.com/science/article/pii/0550321384904528.

[11] Michael Fromm et al. "The QCD deconfinement transition for heavy quarks and all baryon chemical potentials". In: *Journal of High Energy Physics* 2012, 42 (Jan. 2012), p. 42. DOI: 10.1007/JHEP01(2012)042. arXiv: 1111.4953 [hep-lat].

[12] Tobias Rindlisbacher and Philippe de Forcrand. "Two-flavor lattice QCD with a finite density of heavy quarks: heavy-dense limit and "particle-hole" symmetry". In: *JHEP* 02 (2016), p. 051. DOI: 10.1007/JHEP02(2016)051. arXiv: 1509.00087 [hep-lat].

[13] Francesca Cuteri et al. "The nature of the Roberge-Weiss Transition in $N_f = 2$ QCD with Wilson Fermions on $N_t = 6$ lattices". In: *PoS* LATTICE2015 (2016), p. 148. DOI: 10.22323/1.251.0148. arXiv: 1511.03105 [hep-lat].

[14] Philippe de Forcrand and Owe Philipsen. "Constraining the QCD phase diagram by tricritical lines at imaginary chemical potential". In: *Phys. Rev. Lett.* 105 (2010), p. 152001. DOI: 10.1103/PhysRevLett.105.152001. arXiv: 1004.3144 [hep-lat].

[15] Michael Fromm et al. "Onset Transition to Cold Nuclear Matter from Lattice QCD with Heavy Quarks". In: *Phys. Rev. Lett.* 110.12 (2013), p. 122001. DOI: 10.1103/PhysRevLett.110.122001. arXiv: 1207.3005 [hep-lat].

[16] K. E. Eriksson, N. Svartholm, and B. S. Skagerstam. "On invariant group integrals in lattice QCD". In: *Journal of Mathematical Physics* 22.10 (1981), pp. 2276–2278. DOI: 10.1063/1.524760. eprint: https://doi.org/10.1063/1.524760. URL: https://doi.org/10.1063/1.524760.

[17] Andreas Halsch. "Some Polyakov loop expectation values with an effective lattice theory". Bachelor's thesis. Goethe Universität Frankfurt, 2015.

Danksagung

Zum Schluss möchte ich noch einigen Personen danken, ohne die diese Arbeit so nicht möglich gewesen wäre. An erster Stelle ist hier mein Professor Owe Philipsen zu nennen, dem ich für die Ermöglichung und Betreuung dieser Arbeit danke. Ein Dank geht auch an meine Freunde Niklas Cichutek, Reinhold Kaiser, sowie Phoenix Shepherd, die mir bei der Korrektur der Arbeit behilflich waren. Zuletzt möchte ich mich insbesondere noch bei meinen Eltern und meiner Familie bedanken, die mich fortwährend bei meinem Physikstudium unterstützt haben.

Selbstständigkeitserklärung

Erklärung nach § 30 (12) Ordnung für den Bachelor- und dem Masterstudiengang

Hiermit erkläre ich, dass ich die Arbeit selbstständig und ohne Benutzung anderer als der angegebenen Quellen und Hilfsmittel verfasst habe. Alle Stellen der Arbeit, die wörtlich oder sinngemäß aus Veröffentlichungen oder aus anderen fremden Texten entnommen wurden, sind von mir als solche kenntlich gemacht worden. Ferner erkläre ich, dass die Arbeit nicht - auch nicht auszugsweise - für eine andere Prüfung verwendet wurde.

Frankfurt, den